

## PHOSPHORUS-31 NMR AS A PROBE FOR PHOSPHOPROTEINS

**Author:** **Thomas L. James**  
 Department of Pharmaceutical Chemistry  
 U.C.S.F. Magnetic Resonance Laboratory  
 University of California  
 San Francisco, California

**Referee:** Chien Ho  
 Department of Biological Sciences  
 Carnegie-Mellon University  
 Pittsburgh, Pennsylvania

## I. INTRODUCTION

In recent years, technological advances in the area of nuclear magnetic resonance (NMR) have enabled the successful application of NMR to a vast number of problems in biochemistry and biology. Among the applications have been some interesting studies of phosphorylated proteins. However, the full power of the NMR arsenal has certainly not been brought to bear on elucidating the structure and function of phosphoproteins. In this chapter, consequently, we will briefly discuss several potentially valuable NMR methods for phosphoprotein investigation, a number of which have not yet been used with phosphoproteins. This will follow a more general presentation of some basics in  $^{31}\text{P}$  NMR which may not be familiar to all readers. Finally, we will review published  $^{31}\text{P}$  NMR studies of phosphorylated amino acids and proteins.

At the outset, we should map the territory to be covered. This discussion will focus on  $^{31}\text{P}$  NMR techniques of potential value in the study of proteins which are covalently phosphorylated. We will not cover studies of the binding of phosphorylated ligands (substrates, inhibitors, coenzymes, or allosteric effectors) to proteins, which have recently been reviewed,<sup>1,2</sup> unless the phosphoryl group is covalently attached to the protein. It should be noted that certain aspects of phosphorylated proteins have also been reviewed by Vogel.<sup>2</sup>

## II. MAGNETIC PROPERTIES OF THE PHOSPHORUS NUCLEUS

## A. NMR Spectral Parameters

The  $^{31}\text{P}$  isotope of phosphorus occurs naturally to the extent of 100%. This is propitious since  $^{31}\text{P}$  nuclei are among the roughly half of known nuclei which possess a magnetic moment, thus rendering themselves available for NMR studies to probe their environment. More fortunate yet are we since  $^{31}\text{P}$  is one of the most readily detected nuclei, being 6.6% as sensitive as  $^1\text{H}$ . Further advantage occurs since  $^{31}\text{P}$  has a nuclear spin quantum number  $I$  of  $1/2$  and, consequently, does not suffer the complexities due to the quadrupole moment which all nuclei with  $I > 1/2$  possess.

In the following, we will discuss some of the basic NMR parameters of  $^{31}\text{P}$ . The area under a  $^{31}\text{P}$  resonance signal can also be considered as an NMR parameter; it should be noted that, under appropriate experimental conditions, the intensity (area) of an NMR signal is directly proportional to the number of nuclei contributing to that signal. In other words, the integrated resonance intensity can be used to determine the concentration of a particular type of phosphorus. A complete introduction to NMR parameters can be found in the book by James.<sup>3</sup>

### 1. Chemical Shift

The frequency required to induce a phosphorus nucleus to resonate, i.e., produce an NMR signal, depends upon the electronic environment around the nucleus, which can cause a slight perturbation of the effective magnetic field,  $B_{\text{eff}}$ , perceived by the nucleus. The resonance frequency is proportional to the effective magnetic field strength:

$$\nu = \gamma B_{\text{eff}}/2\pi \quad (1)$$

where  $\gamma$  is the gyromagnetic ratio ( $= 10830 \text{ rad/gauss for } ^{31}\text{P}$ ). Consequently, it is often said that a resonance occurs at a higher field if the electronic environment is such that a higher radiofrequency,  $\nu$ , must be applied in order for a phosphorus signal to be produced. The resonance frequency (chemical shift) of a nucleus is expressed relative to that of a reference (85% phosphoric acid here, unless specified otherwise), the units being parts per million obtained by dividing the difference between the reference signal and the interesting signal frequencies (in hertz) by the spectrometer operating frequency (in megahertz).

There are several potential influences on the electronic environment of a phosphorus nucleus, and most of these influences are interdependent. Consequently, the theory of  $^{31}\text{P}$  chemical shifts is not entirely worked out. Contributing factors are the nature and number of atoms attached to the phosphorus, the type of bonding entailed, and the detailed geometry of those bonds. In the case of phosphoproteins, four atoms are bonded to phosphorus with three or four being oxygen and none or one being nitrogen. The presence of attached nitrogen causes chemical shifts a few parts per million upfield. Gorenstein<sup>4</sup> has theoretically demonstrated the influence of bond angles and coupled torsion angles on the  $^{31}\text{P}$  chemical shift, which was corroborated experimentally. The experimental demonstration that the solvent influences chemical shifts of phosphates<sup>5</sup> has implications for phosphoproteins because the phosphorus residue may be either on the surface of the protein in a hydrophilic environment or buried in the hydrophobic environment of the protein. In such a hydrophobic environment, of course, using current effects from aromatic side chains can affect the chemical shift of the phosphorus residue. As we will see later, the  $^{31}\text{P}$  chemical shift of a native phosphoprotein can be altered by denaturation.

Variations of pH in the range of the  $\text{pK}_a$  of the phosphoryl moiety can influence the  $^{31}\text{P}$  chemical shift. This will occur only if the phosphoryl moiety is accessible to solvent. Raising the pH such that a dianion is formed from a monoanion causes a downfield shift of 4 ppm for phosphomonoesters ( $\text{R-O-PO}_3^-$ ), 5 ppm for acylphosphates ( $\text{R-COO-PO}_3^-$ ), and 2.5 ppm for phosphoramidates ( $\text{R-NH-PO}_3^-$ ).<sup>6</sup> Of course, disubstituted phosphoryl groups cannot form a dianion and the chemical shift position will not titrate with pH. The lack of pH dependence of a  $^{31}\text{P}$  resonance peak for an accessible phosphorus residue is evidence that it is disubstituted.<sup>7</sup> Gassner et al.<sup>8</sup> have found that the phosphohistidine  $^{31}\text{P}$  resonance also does not titrate very much. However, a phosphohistidine and a disubstituted phosphorus residue can often be distinguished by the lack of  $^{31}\text{P}$ - $^1\text{H}$  spin-spin splitting (*vide infra*) in the phosphohistidine.

The observed  $\text{pK}_a$  of the phosphorus residue may provide some information about its environment relative to that of the free phosphoamino acid. Formation of salt bridges and the nature of proximal groups in the protein are expected to vary the pH titration curve of the  $^{31}\text{P}$  resonance.<sup>9</sup>

Just as proteolysis causes the  $^{31}\text{P}$  resonance to move, complex formation with cations can result in resonance shifts. Complex formation with diamagnetic cations will cause a shift of at most a couple parts per million, but binding of paramagnetic metal ions can result in much larger shifts.<sup>3</sup>

## 2. Coupling Constant

Nuclei with magnetic moments, such as  $^{31}\text{P}$ , can interact via intervening bonds with other nuclei possessing magnetic moments, such as  $^1\text{H}$ .<sup>3</sup> This interaction is independent of magnetic field strength and leads to splitting of the resonance peaks for small molecules. For most native phosphoproteins, this spin-spin splitting is not resolved in the  $^{31}\text{P}$  resonance, but it results in broadening of the observed resonance. The existence of this scalar spin-spin coupling between phosphorus and protons can be demonstrated by narrowing of the phosphorus peak when the protons are decoupled by strong irradiation at their resonance frequency. The actual value of the coupling constant  $J_{\text{P-OCH}}$  in phosphoesters has been shown to be dependent on the dihedral angle<sup>10</sup> as theoretically predicted by Karplus.<sup>3</sup> However, bond rotation in nonrigid systems of interest will yield coupling constant values time-averaged between all allowed conformations.

Although it has not yet been reported, it may even be possible to extract  $^{31}\text{P}$ - $^1\text{H}$  coupling constants from the  $^{31}\text{P}$  resonance of a phosphoprotein with unresolved coupling between P-O-CH<sub>2</sub>. The outer two components in the unresolved  $^{31}\text{P}$  triplet, caused by coupling to the two protons, can be inverted in a Fourier transform spin echo experiment leaving the central component upright (see Reference 3, p. 163). With a sufficient amount of compound,  $^{31}\text{P}$ - $^1\text{H}$  scalar coupling can also be observed using two-dimensional NMR techniques.<sup>11</sup>

## 3. Relaxation

After a sample has absorbed energy at the frequency appropriate for phosphorus to resonate, the system of phosphorus nuclei proceed to disseminate that energy in an attempt to relax toward the thermal equilibrium state which can be achieved in the absence of any phosphorus-exciting radiation. There are two different types of relaxation: (1) spin-spin relaxation with a time constant  $T_2$ ; and (2) spin-lattice relaxation with a time constant  $T_1$ . Both relaxation processes are affected by interactions of the nuclear magnetic moment with rapidly fluctuating magnetic fields.<sup>3</sup> In the case of  $^{31}\text{P}$ , the fluctuating magnetic fields effective in causing relaxation usually are produced by the magnetic moments of other nearby nuclei (generally protons) or by the chemical shift anisotropy tensor. The magnetic fields fluctuate due to Brownian motion (both rotational and translational) of molecules in the sample.

We can write expressions for the  $^{31}\text{P}$  relaxation parameters via the heteronuclear dipole-dipole (DD) and chemical shift anisotropy (CSA) mechanisms. The selective DD relaxation rates (obtained in the presence of proton decoupling) for  $^{31}\text{P}$  coupled to a single hydrogen are given by<sup>12</sup> Equations 2 to 4:

$$(1/T_1)_{\text{DD}} = K[J_{\text{DD}}(\omega_{\text{H}} - \omega_{\text{P}}) + 3J_{\text{DD}}(\omega_{\text{P}}) + 6J_{\text{DD}}(\omega_{\text{H}} + \omega_{\text{P}})] \quad (2)$$

$$(1/T_2)_{\text{DD}} = (1/2T_1)_{\text{DD}} + K[2J_{\text{DD}}(0) + 3J_{\text{DD}}(\omega_{\text{H}})] \quad (3)$$

$$(\text{NOE})_{\text{DD}} = 1 + \frac{\gamma_{\text{H}}}{\gamma_{\text{P}}} \frac{6J_{\text{DD}}(\omega_{\text{H}} + \omega_{\text{P}}) - J_{\text{DD}}(\omega_{\text{H}} - \omega_{\text{P}})}{J_{\text{DD}}(\omega_{\text{H}} - \omega_{\text{P}}) + 3J_{\text{DD}}(\omega_{\text{P}}) + 6J_{\text{DD}}(\omega_{\text{H}} + \omega_{\text{P}})} \quad (4)$$

where  $T_1$  and  $T_2$  are the spin-lattice and spin-spin relaxation times, respectively, and NOE is the nuclear Overhauser enhancement of the signal intensity relative to the signal obtained without broadband proton irradiation;  $\gamma_{\text{H}}$  (26750 rad/gauss) and  $\gamma_{\text{P}}$  (10830 rad/gauss) are the gyromagnetic ratios, and  $\omega_{\text{H}}$  and  $\omega_{\text{P}}$  are the Larmor frequencies of hydrogen and phosphorus, i.e.,  $2\pi$  times the spectrometer frequency. The  $J(\omega)$  terms are the spectral densities of molecular motion, and the constant  $K$  is given by

$$K = (\hbar^2 \gamma_{\text{P}}^2 \gamma_{\text{H}}^2) / (20r^6) \quad (5)$$

where  $r$  is the proton-phosphorus internuclear distance.

In the case of CSA relaxation, the relevant equations are

$$(1/T_1)_{\text{CSA}} = (6/40)\omega_p^2\delta_z^2[1 + (\eta^2/3)]J_{\text{CSA}}(\omega_p) \quad (6)$$

and

$$(1/T_2)_{\text{CSA}} = (1/40)\omega_p^2\delta_z^2[1 + (\eta^2/3)][3J_{\text{CSA}}(\omega_p) + 4J_{\text{CSA}}(0)] \quad (7)$$

Here  $\delta_z$  is the anisotropy and  $\eta$  the asymmetry of the chemical shift tensor. In the presence of both relaxation mechanisms, the combined relaxation rates are given by

$$1/T_{1,2} = (1/T_{1,2})_{\text{DD}} + (1/T_{1,2})_{\text{CSA}} \quad (8)$$

and

$$\text{NOE} = 1 + (\text{NOE}_{\text{DD}} - 1)[T_1/(T_1)_{\text{DD}}] \quad (9)$$

Analytical expressions for the spectral densities are based upon models for molecular motion. In the case of isotropic rotation characterized by a single correlation time,  $\tau_c$ , the spectral densities are

$$J_{\text{DD}}(\omega) = J_{\text{CSA}}(\omega) = (2\tau_c)/(1 + \omega^2\tau_c^2) \quad (10)$$

The assumption of only a single isotropic tumbling motion is probably an oversimplification in most cases; more complicated molecular motions and relaxation will be discussed below.

It is important to note that the signal line width  $W_{1/2}$  is related to  $T_2$  by

$$W_{1/2} = 1/\pi T_2 \quad (11)$$

This relationship holds in the absence of magnetic field inhomogeneity, which in practice is usually satisfactory as long as  $T_2 \lesssim 0.5$  sec.

Table 1 lists the CSA values for a series of model compounds, thus providing a starting point for CSA calculations with phosphoproteins. It may be noted that protonating a phosphoryl group has the effect of increasing the CSA.

For most purposes, an undesirable mechanism of relaxation is provided by paramagnetic ions. For that reason, efforts should be made to remove any paramagnetic metal ions from the sample.

It was recently demonstrated by Bendel and James<sup>18</sup> that another relaxation mechanism, that of scalar relaxation of the second kind,<sup>3</sup> may dominate the spin-spin relaxation ( $T_2$ ) process of  $^{31}\text{P}$  in phosphoryl groups in which the phosphorus is scalar-coupled to protons. To eliminate this mechanism from contributing to the  $T_2$  relaxation process and, consequently, to  $^{31}\text{P}$  line widths, it is recommended that decoupling of the protons be employed.

## B. Techniques for Phosphoproteins

As already mentioned, the techniques of proton decoupling and pH variation can provide information about the nature of the phosphoryl group, the environment around the group, and the accessibility of the group to water. Here we will consider some other techniques which have potential applicability to the investigation of phosphoproteins, some which have already been utilized and others which have not. Of course, the reader is cautioned that any previously untried experiments may prove more difficult to apply than is implied by suggestions made here. Readers wishing simply to review what NMR studies have already

**Table 1**  
**<sup>31</sup>P CHEMICAL SHIFT ANISOTROPY AND**  
**ASYMMETRY VALUES FOR MODEL COMPOUNDS**

Compound	δ <sub>z</sub> (ppm)	η (ppm)	Ref.
Phosphomonoesters			
Phosphoserine	51	-0.8	13
Phosphoserine, acid	66	-1.1	14
Phosphorylethanolamine	73	-0.7	13
5'-AMP, disodium	71	0	15
5'-AMP, acid	84	-0.8	15
5'-GMP, disodium	59	0	15
3'-CMP, acid	83	-0.8	15
Phosphodiester			
L-α-Glycerolphosphoryl choline	86	-0.6	13
A-DNA, sodium salt	102	-0.6	16
Diethylphosphate, barium salt	104	-0.5	17
Dipalmitoylphosphatidylethanolamine	104	-0.6	17
Dipalmitoylphosphatidylcholine	111	-0.5	17
3',5'-CMP, sodium	125	-0.4	14
3',5'-CMP, acid	140	-0.6	14
Acyl phosphates			
Acetyl phosphate	103	-2.9	14
Phosphoramidates			
Imidazole diphosphate	105	-2.6	14
Phosphocreatine	125	-2.1	14

contributed to understanding phosphoproteins are advised to skip this section and go to Section III.

### 1. Paramagnetic Probes and Water Accessibility

The presence of a paramagnetic ion, such as Mn(II), in solution can cause line broadening and T<sub>1</sub> alterations for nuclei which are near the Mn(II), due to the electron spin relaxation mechanism.<sup>3</sup> Consequently, it is possible to use the Mn(II) as a probe to discover if a phosphoryl group on a phosphoprotein is near the surface or is buried.<sup>19</sup> (It is presumed that the protein has not enveloped the Mn(II) and that it is bound at the surface or is free in solution.) The extent of line broadening is strongly related to the distance, *r*, between Mn(II) and <sup>31</sup>P (see Equation 12 below), so a phosphorus at the surface could have its resonance broadened beyond detection while the resonance of a buried phosphate may be little affected by the paramagnetic ion. The paramagnetic effect can also be utilized to learn about the proximity of a phosphorus residue to a group on the enzyme which can be made paramagnetic, e.g., the semiquinone form of a coenzyme.<sup>7</sup>

Under favorable conditions, the unpaired electron-phosphorus distance, *r* (in cm), can be estimated from the paramagnetic contribution to the line width (Reference 3, Equations 6 to 13 modified):

$$(W_{1/2})_{para} = \frac{6.435 \times 10^{-34}}{r^6} \left( 4\tau_c + \frac{3\tau_c}{1 + \omega_p^2 \tau_c^2} + \frac{13\tau_c}{1 + 2.64 \times 10^6 \omega_p^2 \tau_c^2} \right) \quad (12)$$

where ω<sub>p</sub> is 2π times the <sup>31</sup>P spectrometer frequency and τ<sub>c</sub>, the correlation time for the motion modulating the electron-phosphorus dipolar interaction, can be experimentally determined or estimated.<sup>3</sup>

Another possible way to monitor accessibility of a phosphoryl group to water is via cross-relaxation. This method has not been employed. Basically, the experiment is to see if the phosphorus resonance intensity changes when the water proton resonance is irradiated. The

*caveat* in this experiment is that one must be aware of the possibility of irradiating the resonances of protein protons near the phosphorus. Furthermore, complications may arise from spin diffusion among all the protons in the sample if the pulse sequence timing is too long. Cross-relaxation between water protons and protein protons has been discussed by Fung and McGaughy.<sup>20</sup>

## 2. Molecular Motions

As mentioned previously, the NMR relaxation parameter values are dependent upon molecular motions. In fact, NMR relaxation parameter measurements can be used to investigate molecular motions, overall as well as internal motions. The NMR can therefore be used to characterize the phosphoryl group dynamics and alterations in those dynamics as conditions of the phosphoprotein are modified.

As noted above, the assumption of a single isotropic motion is clearly an oversimplification for macromolecules such as phosphoproteins, and indeed, relaxation data that consist of more than one measured parameter for such molecules can rarely be fit to theory by assuming a single correlation time. Therefore, additional degrees of freedom with freely variable correlation times are usually introduced by means of various models. In these models a fast internal motion is usually superimposed on the slower, overall reorientation of the phosphoprotein molecule. Frequencies for the internal motion can usually be obtained readily with some idea of the amplitude of motion also being garnered. A detailed discussion of the use of <sup>31</sup>P NMR relaxation measurements to study molecular motions has recently been presented.<sup>21</sup> The CSA parameters listed in Table 1 can be used in such a study.

Although the approaches can entail relatively sophisticated calculations,<sup>21</sup> a fairly straightforward model which at least yields motional frequencies comparable to those of more exacting calculations is provided by Woessner's model for free internal diffusion about an axis that itself undergoes isotropic reorientation. In this approach, both the overall and the internal motion correlation times are allowed to vary and the spectral densities for the dipolar interaction to be used in Equations 2 to 4 are given by Equations 13 to 18:

$$J_{\text{DD}}(\omega) = A \frac{2\tau_0}{1 + \omega^2\tau_0^2} + B \frac{2\tau_B}{1 + \omega^2\tau_B^2} + C \frac{2\tau_C}{1 + \omega^2\tau_C^2} \quad (13)$$

$$A = \frac{1}{4}(3 \cos^2 \phi - 1)^2 \quad (14)$$

$$B = \frac{3}{4} \sin^2 2\phi \quad (15)$$

$$C = \frac{3}{4} \sin^4 \phi \quad (16)$$

$$\tau_B = [1/\tau_0 + 1/(6\tau_i)]^{-1} \quad (17)$$

$$\tau_C = [1/\tau_0 + 2/(3\tau_i)]^{-1} \quad (18)$$

where  $\tau_0$  and  $\tau_i$  are the correlation times for the overall and internal motions, respectively, and  $\phi$  is the angle between the phosphorus-hydrogen internuclear vector and the axis of internal rotation. The analogous equations for the spectral densities of the CSA mechanism, to be used in Equations 6 and 7, are

$$J_{\text{CSA}}(\omega) = \frac{1}{(1 + (\eta^2/3))} \sum_{j=0}^2 C_j \frac{2\tau_j}{1 + \omega^2\tau_j^2} \quad (19)$$

Here  $\tau_0$ ,  $\tau_1$ , and  $\tau_2$  are, respectively, identical with  $\tau_0$ ,  $\tau_B$ , and  $\tau_C$  in the dipolar case, and the geometrical coefficients are given in Equations 20 to 22, where  $\beta$  and  $\gamma$  are the Euler angles rotating the



$$C_0 = 1/4[(3 \cos^2 \beta - 1) + \eta \sin^2 \beta \cos 2\gamma]^2 \quad (20)$$

$$C_1 = 1/3 \sin^2 \beta [\cos^2 \beta (3 - \eta \cos 2\gamma)^2 + \eta^2 \sin^2 2\gamma] \quad (21)$$

$$C_2 = [(3/4)^{1/2} \sin^2 \beta + [\eta/2(3^{1/2})](1 + \cos^2 \beta) \cos 2\gamma]^2 \\ + (\eta^2/3) \sin^2 2\gamma \cos^2 \beta \quad (22)$$

coordinate system of the internal rotational diffusion into the CSA principal axis system.

### 3. Isotopic Substitution

Certain aspects of the chemistry of the phosphoryl group in phosphoproteins can be examined by isotopic substitution. For example, the  $^{31}\text{P}$  NMR relaxation time can be modified and spin-spin splitting virtually eliminated when the protons affecting the interactions are replaced by deuterons. The replacement of the protons in the phospho-amino acid residue causing spin-spin splitting may not be easy experimentally. Changing solvent isotopic composition is easy, and water protons do sometimes contribute to  $^{31}\text{P}$  relaxation.

The chemistry of phosphoryl transfer reactions has been examined by monitoring the influence of  $^{18}\text{O}$  or  $^{17}\text{O}$  isotopes (relative to  $^{16}\text{O}$ ) on the  $^{31}\text{P}$  resonance.<sup>22</sup> However, the effect of oxygen isotopes on the  $^{31}\text{P}$  NMR of phosphoproteins has not yet been exploited. The  $^{18}\text{O}$  isotope bonded to phosphorus causes a small change in the  $^{31}\text{P}$  resonance frequency. The shift would be too small to be observed with the intact phosphoprotein due to the relatively broad  $^{31}\text{P}$  resonance signal, but shifts should be discernible with smaller phosphopeptides. The  $^{17}\text{O}$  isotope has a quadrupole moment and, consequently, provides a very efficient relaxation mechanism (scalar coupling of the second kind<sup>3,12</sup>) for  $^{31}\text{P}$  when  $^{17}\text{O}$  is directly bonded. Experiments which result in  $^{17}\text{O}$  being attached to the phosphorus may result in a  $^{31}\text{P}$  resonance which becomes broadened due to an additional relaxation mechanism. The line width for this scalar relaxation mechanism is given by<sup>3</sup>

$$(W_{1/2})_1 = \frac{4\pi^2 J^2 I_2(I_2 + 1)}{3} \left[ (T_1)_2 + \frac{(T_2)_2}{1 + (\omega_1 - \omega_2)^2 (T_2)_2^2} \right] \quad (23)$$

where  $I$  is the spin quantum number,  $J$  is the scalar coupling constant,  $\omega$  is  $2\pi$  times the spectrometer frequency, and the subscripts 1 and 2, respectively, refer to the nucleus being studied (e.g.,  $^{31}\text{P}$ ) and the nucleus scalar-coupled to it (e.g.,  $^{17}\text{O}$ ). This scalar relaxation mechanism is usually most important if the scalar-coupled nucleus possesses a quadrupole moment and, consequently, has an efficient relaxation mechanism itself.

An interesting observation of  $^{31}\text{P}$  resonances for phosphorus-containing ligands with  $^{17}\text{O}$  bonded has been made in the situation where the ligand is bound to a protein. However, with the free ligand, the  $^{31}\text{P}$  resonance was broadened beyond detection. The rationale for this observation is apparent from Equation 23. The bound ligand will have much smaller  $(T_1)_1$  and  $(T_2)_2$  values for  $^{17}\text{O}$  due to its quadrupolar relaxation mechanism.<sup>3</sup> This will diminish the importance of the scalar relaxation contribution (Equation 23) for phosphorus on the macromolecule. But the resonance will be broader with  $^{17}\text{O}$  attached than with  $^{16}\text{O}$  attached.

### 4. Two-Dimensional NMR

To date, 2D NMR techniques have not been applied to phosphoproteins, but they probably will be in the future. The 2D NMR experiments are very time-consuming and require a high concentration of sample; at a minimum, concentrations of a couple millimolars will be required. Bolton<sup>11</sup> has already illustrated the applicability of 2D NMR on heteronuclear scalar interactions between phosphorus and protons in phosphoserine.

Basically, 2D NMR experiments provide a means of examining the consequences of internuclear interactions, both scalar and dipole-dipole interactions. The basic experimental

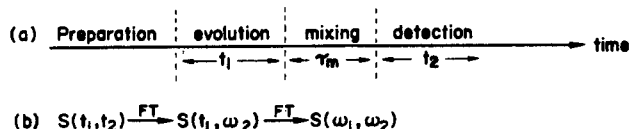


FIGURE 1. (a) Time-course of a generalized 2D NMR experiment. The preparation period generally entails an initial delay time followed by an RF pulse or pulses. Following the perturbation, the nuclear spin system evolves for a time,  $t_1$ , which is incrementally varied as the whole sequence is repeated a number of times. For some experiments, a constant mixing time  $\tau_m$ , which may include pulses, follows. Finally, the free induction decay signal  $S(t_1, t_2)$  is acquired for a length of time,  $t_2$ , just as in ordinary Fourier transform NMR. (b) Several free induction decay (FID) signals  $S(t_1, t_2)$  will be acquired, one for each value of  $t_1$  employed. The first Fourier transform will be carried out over the acquisition period  $t_2$  of each FID as in ordinary FT NMR, yielding a series of spectra  $S(t_1, \omega_2)$  related by the  $t_1$  increment. The second Fourier transform is over the  $t_1$  which sequentially varies in each  $S(t_1, \omega_2)$  to give the second frequency dimension in the final 2D NMR spectrum  $S(\omega_1, \omega_2)$ .

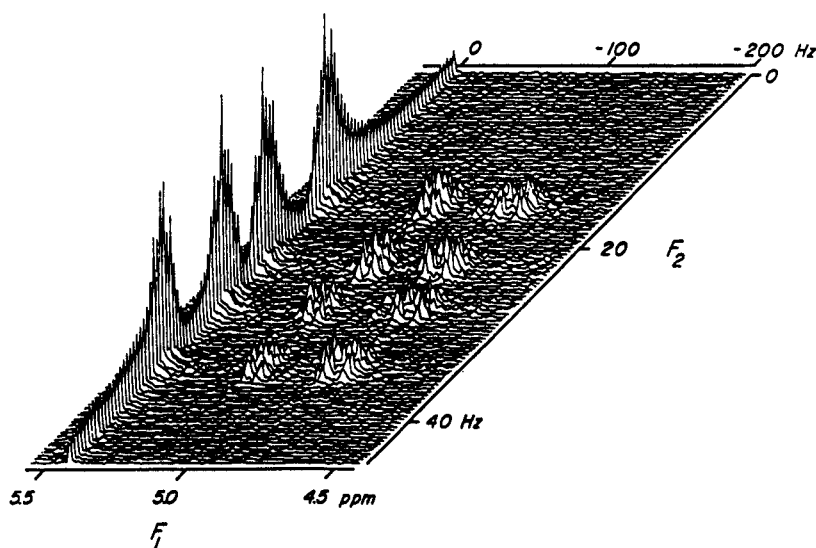


FIGURE 2. Heteronuclear 2D spectrum of 2',3'-cUMP (0.2 M, 40%  $^2\text{H}_2\text{O}$ /60%  $\text{H}_2\text{O}$ , pH 7.5, 35°C) with a phosphorus frequency of 81 MHz and proton frequency of 200 MHz. The evolution time,  $t_1$ , was incremented in 256 steps of 2.5 msec each.  $F_1$  is the proton frequency domain and  $F_2$  is the phosphorus frequency domain. The projection onto the  $F_1 = 0$  Hz axis represents the one-dimensional  $^{31}\text{P}$  spectrum. (From Bodenhausen, G. and Bolton, P. H., *J. Magn. Reson.*, 39, 399, 1980. With permission.)

protocol is illustrated in Figure 1. There are various sequences which vary in detail, depending to some extent on whether one wishes a 2D NMR spectrum expressing the strength of scalar coupling as a function of peak chemical shift (J-spectroscopy), correlating the chemical shifts of scalar-coupled nuclei (shift correlation spectroscopy), manifesting multiple quantum transitions (2D multiple quantum spectroscopy), or correlating the chemical shifts of dipolar-coupled nuclei (2D nuclear Overhauser effect (NOE) spectroscopy). The monograph of Bax<sup>24</sup> describes many of these 2D NMR experiments. Macura and Ernst<sup>25</sup> discuss 2D NOE spectroscopy.

An example of a moderately complicated heteronuclear 2D spectrum is shown in Figure 2.<sup>26</sup> The H2' and H3' protons of 2',3'-cUMP together with the phosphorus form an AMX spin system which shows up in the 2D spectrum. The  $F_1$  frequency domain is that of  $^1\text{H}$



and the  $F_2$  frequency is that for  $^{31}\text{P}$ . The signals at 5.14 and 4.92 ppm are due to  $\text{H2}'$  and  $\text{H3}'$ , respectively. The projection shown at  $F_1 = 0$  Hz is the one-dimensional  $^{31}\text{P}$  spectrum expected when  $J(\text{H2}'\text{-P}) = 6.9$  Hz and  $J(\text{H3}'\text{-P}) = 11.5$  Hz. However, the second dimension permits the individual  $\text{H2}'$  and  $\text{H3}'$  signals to be separated. Additional splittings in the  $F_1$  dimension are due to  $J(\text{H1}'\text{-H2}') = 3.0$  Hz and  $J(\text{H3}'\text{-H4}') = 5.5$  Hz.

### 5. Molecular Structure from Relaxation and 2D NMR

To date,  $^{31}\text{P}$  NMR relaxation parameters have not been used to examine structural details in phosphoproteins. In principle, however, they could be utilized. Proton NMR relaxation parameters, in particular the nuclear Overhauser effect (NOE), have been used to obtain structural information on small molecules.<sup>27</sup> With the small size of the molecules, extreme narrowing conditions ( $\omega\tau_c \ll 1$ ) generally apply so the spectral densities are particularly simple. In the case of macromolecules, the situation may also be simple under certain conditions. With a two-spin system entailing a  $^{31}\text{P}$  and a  $^1\text{H}$  nucleus, and dipolar relaxation via interaction between the two spins as the only source of relaxation, the  $^{31}\text{P}$  NOE is

$$\text{NOE} = 1 + \frac{\gamma_{\text{H}}^2 \gamma_{\text{P}}^2 \hbar^2}{20r^6} [6J(\omega_{\text{H}} + \omega_{\text{P}}) - J(\omega_{\text{H}} - \omega_{\text{P}})]T_1 \quad (24)$$

which follows from Equations 2 and 4. This expression allows the P-H distance,  $r$ , to be determined readily from the  $^{31}\text{P}$  NOE and  $T_1$  measurement if the spectral densities can be determined. The problem is that this case of a single dipole-dipole interaction being the only source of relaxation is unusual in systems of interest. In addition, extensive self-diffusion among the protons can make the situation more complicated.<sup>28</sup>

Measurements of transient NOE values rather than steady-state NOE values can circumvent some of the problems. Bothner-By and Noggle<sup>29</sup> computed the time development of the NOE in a multispin system; that approach has been used to study proton-proton interactions in lysozyme.<sup>30</sup> So far, such experiments have not been conducted in heteronuclear systems.

Spin-lattice relaxation time measurements may also yield distance data. This entails a combination of nonselective, semiselective, and selective relaxation time measurements. In each case, initial relaxation rates are measured. The nonselective  $T_1$  measurement is the usual inversion recovery experiment<sup>3</sup> in which the  $180^\circ$  pulse is simultaneously applied to all interacting nuclei. Only one nucleus is subjected to the inverting  $180^\circ$  pulse in the selective  $T_1$  measurement, and only two nuclei in the biselective experiment. The initial  $T_1$  values may vary in these three experiments and may be shown to give<sup>31</sup>

$$(1/T_1)_j^{\text{ns}} = (1/T_1)_j^{\text{s}} + \sum_i \frac{\gamma_i^2 \gamma_j^2 \hbar^2}{20r_{ij}^6} [6J(\omega_{\text{H}} + \omega_{\text{P}}) - J(\omega_{\text{H}} - \omega_{\text{P}})] \quad (25)$$

$$(1/T_1)_j^{\text{bs}} = (1/T_1)_j^{\text{s}} + \frac{\gamma_i^2 \gamma_j^2 \hbar^2}{20r_{ij}^6} [6J(\omega_{\text{H}} + \omega_{\text{P}}) - J(\omega_{\text{H}} - \omega_{\text{P}})] \quad (26)$$

where the initial relaxation of nucleus  $j$  is measured in the selective (superscript s), non-selective (superscript ns), and biselective (superscript bs) experiment. In the  $(1/T_1)_j^{\text{ns}}$  expression, the sum is over all nuclei  $i$  which are dipolar-coupled to nucleus  $j$ ; subscript  $i$  in the  $(1/T_1)_j^{\text{bs}}$  expression refers to the particular nucleus whose spin is also inverted in the biselective experiment. This method should be valid even when other relaxation mechanisms (such as chemical shift anisotropy) contribute to  $^{31}\text{P}$  relaxation since these other contributions will appear in  $(1/T_1)^{\text{s}}$ .

Another relaxation technique which is likely to see much utilization for structural studies in the future is the 2D NOE experiment mentioned above. The basic experiment entails the pulse sequence  $[(\pi/2)_x - t_1 - (\pi/2)_x - \tau_{\text{M}} - (\pi/2)_x - t_2 - ]$  which yields a 2D spectrum following the double Fourier transformation (*vide supra*). The intensity of a peak in the 2D NOE spectrum arising from interaction of nucleus  $j$  with nucleus  $k$  is<sup>25</sup>

$$[\text{Intensity}]_{jk} \propto C[\exp(-R\tau_M)]_{jk} \quad (27)$$

where  $\tau_M$  is the experimental mixing time, and the relaxation matrix,  $R$ , is composed of transition probability terms which are proportional to  $J(\omega)/r_{jk}^6$ . There have been some difficulties with phasing 2D spectra, the appearance of cross-peaks due to scalar coupling, and the relatively long time required for an experiment; however, these problems are being overcome to a certain extent. The technique holds considerable promise with the possibility of determining solution structures with a resolution approaching that for crystals by X-ray diffraction. This potential should be considerably augmented by the use of the distance geometry algorithm.<sup>32</sup> So far, only proton homonuclear 2D NOE experiments have been used in a qualitative (or perhaps semiquantitative) sense to obtain structural information from proteins.<sup>33,34</sup>

## 6. Solid-State NMR

Solid-state NMR techniques have not been widely utilized to elucidate the environment or mobility of the phosphoryl groups in phosphoproteins. One  $^{31}\text{P}$  NMR study has been carried out with a crystalline lipovitellin-phosvitin complex.<sup>35</sup> In comparison, some of the experimental solid-state NMR techniques have seen somewhat wider applicability with other spin  $-1/2$  nuclei such as in recent  $^1\text{H}$ ,  $^{13}\text{C}$ , and  $^{15}\text{N}$  NMR investigations of proteins.

In solution, the fast molecular tumbling will usually result in the rapid reorientation of magnetic dipole vectors and chemical shift anisotropy (CSA) tensors, with respect to the stationary magnetic field. However, in solids or other relatively immobile systems such as proteins in membranes or in large macromolecular assemblies, the dipole-dipole interactions (principally due to nearby protons) and the CSA may not be averaged out by molecular motions. Under these circumstances, broad signals (typically  $>40$  kHz), which may also be asymmetric if CSA is a factor, will result using ordinary Fourier transform NMR methods. In fact, the signals may be so broad that detection becomes difficult.

Just as scalar  $^{31}\text{P}$ - $^1\text{H}$  interactions which have a strength  $<100$  Hz can be squelched by applying a sufficiently strong radiofrequency (RF) field ( $\gamma B/2\pi \approx 1$  kHz) at the proton resonance frequency, the dipolar  $^{31}\text{P}$ - $^1\text{H}$  interactions can be suppressed by application of a RF field to the protons, only the irradiation must be much stronger (e.g.,  $\gamma B/2\pi \sim 60$  kHz) to work since the dipolar interactions are so much stronger than the scalar interactions.<sup>36</sup> Since the dipolar interaction depends on the orientation of the P-H vector in the field of the laboratory magnet, the anisotropy of the rotational motion as well as the frequency of that motion influences the line broadening in the absence of dipolar decoupling. There have been various lineshape analyses in terms of molecular motions which provide information about molecular motions in the millisecond time range. The lineshape in the dipolar-decoupled spectrum still exhibits CSA which can yield structural data.

Further line narrowing can be obtained by removing the effects of CSA via magic angle sample spinning (MASS). Although for some experiments it is worthwhile to use MASS or dipolar decoupling independently, the line-narrowing objectives of each experiment are made easier in a combination of the two experiments since one technique decreases the line width enough to make it easier for the other to operate.

CSA will exist as long as the chemical shielding is not equal in all directions around the nucleus and the rotations are not fast enough to average the shielding (as they are in liquids). The CSA is represented by a tensor with a factor  $(3\cos^2\Theta - 1)$ ; the CSA interactions therefore can be suppressed by rotating the sample at the "magic angle"  $\Theta = 54.74^\circ$  with respect to the laboratory magnet as long as the rate of rotation is greater than the strength of the interaction, typically a few kilohertz. If there is already some molecular motion, it may be necessary to spin even faster to effect further reduction in line width due to CSA. At intermediate rates of rotation, series of spinning side bands occur which can be used to obtain information about the CSA.<sup>37</sup>

Even with MASS and dipolar decoupling, the sensitivity of the experiments could stand to be enhanced considerably, primarily due to the long  $T_1$  values for nuclei in a rigid environment. A method, appropriate for  $^{13}\text{C}$ ,  $^{15}\text{N}$ , and  $^{31}\text{P}$ , entailing polarization transfer from the abundant protons to the "rare" nuclei of interest can, in principle, lead to a sensitivity enhancement of  $\gamma_{\text{H}}/\gamma_{\text{I}}$  (in practice, around 70% of this is usually achieved) and, even more importantly, permit sequence repetition rates based on the faster proton  $T_1$ .<sup>35</sup> The cross-polarization technique was initiated by Hartmann and Hahn, but did not gain many advocates until after the work of Pines et al.<sup>38</sup> For polarization transfer to work, the Hartmann-Hahn condition, i.e.,  $\gamma_{\text{I}}H_{\text{I}}(\text{I}) = \gamma_{\text{H}}H_{\text{I}}(\text{H})$ , must be achieved. This is not necessarily easy experimentally, but several variants have been used such that the match can be made and polarization transfer effected.<sup>35</sup>

Such experiments commonly include dipolar decoupling as well as cross-polarization. The length of time for the Hartmann-Hahn contact can be varied and the rate of polarization transfer measured.<sup>35</sup> The proton  $T_{1\rho}$  also can be determined from this and motional data thus derived. Variation of the contact time enables the selective enhancement of resonances in the spectrum according to the degree of rigidity since, as the contact time is increased, the signals will initially increase in amplitude and then decrease with rates being determined by the strength of the dipolar interaction and the proton  $T_{1\rho}$ .

A combination of the solution-state and solid-state NMR experiments should enable a more complete characterization of complicated systems such as macromolecular assemblies containing phosphoproteins where some portions may be relatively rigid and other relatively free. Three techniques can serve to distinguish between the rotationally mobile and immobile portions: (1) scalar decoupled experiment (typical FT NMR); (2) cross-polarization experiment; and (3) dipolar decoupling experiment. MASS may or may not be used in conjunction with the latter two. The first experiment will detect the rotationally mobile moiety, the second will detect the immobilized portion, and the third will detect both free and immobilized portions.

### III. NMR STUDIES OF PHOSPHORYLATED AMINO ACIDS AND PEPTIDES

The  $^{31}\text{P}$  chemical shifts of phosphorylated amino acids as well as several other biological compounds are listed in Table 2. In the first study of phosphoproteins, Ho et al.<sup>46</sup> observed the  $^{31}\text{P}$  NMR of *phosphoserine* and *phosphothreonine*. As noted in Table 2, phosphoserine and phosphothreonine have somewhat different chemical shifts, and the pH dependence of their  $^{31}\text{P}$  chemical shifts are similar with  $\text{pK}_a$  values of 5.8 and 5.9, respectively. Their resonances do differ in that the methylene protons cause the phosphorus resonance of phosphoserine to be split into a triplet, but the methine proton produces a doublet in the phosphorus resonance of phosphothreonine.<sup>46</sup> This phosphorus-proton scalar coupling was the basis for using phosphoserine to demonstrate some two-dimensional NMR methods which could prove useful in investigating conformations of biochemical phosphates.<sup>11</sup>

*Phosphotyrosine* is the other phosphomonoester among the phosphorylated amino acids. Although its  $^{31}\text{P}$  resonance shifts upfield 4.0 ppm to  $-3.3$  ppm upon protonation to the monoanionic form, the chemical shifts are found significantly upfield of those for phosphoserine or phosphothreonine (cf. Table 2). No splitting of the phosphorus resonance of phosphotyrosine was evident.<sup>41</sup>

Among the phosphorylated amino acids which are phosphoramidates, only the *phospholysine* resonance has been reported to titrate in the neutral pH range.<sup>40</sup> The  $^{31}\text{P}$  resonance of *phosphoarginine* did titrate with a  $\text{pK}_a$  of 4.3,<sup>6</sup> but  $\text{N}(\pi)$  and  $\text{N}(\tau)$  *phosphohistidines* reportedly did not titrate very much.<sup>8</sup> No spin-spin splitting of  $^{31}\text{P}$  has been reported for this class of phosphorylated amino acids.

As a better model for phosphoproteins, Kalbitzer and Röscher<sup>47</sup> examined the phosphorus

**Table 2**  
**<sup>31</sup>P CHEMICAL SHIFTS OF SOME BIOLOGICAL COMPOUNDS**  
**AT ABOUT pH 7<sup>a</sup>**

Compound	Chemical shift <sup>a</sup> (ppm)	Ref.
Inorganic phosphate	1.7—2.3	39
Inorganic pyrophosphate	— 7.0	39
Phosphonate	~22	39
Polyphosphates	— 22	39
Phosphomonoesters		
Phosphoserine	4.0	40
Phosphothreonine	3.2	40
Phosphotyrosine	0.7	41
Flavin mononucleotide	4.3	7
Pyridoxal phosphate	4.0	39
2-Phosphoglycerate	3.6	39,40
3-Phosphoglycerate	4.2	39
Glucose 6-phosphate	4.2—4.7	39
Dihydroxyacetone phosphate	4.5—5.1	39
O-Phosphoethanolamine	3.7	40
Phosphoenolpyruvate	— 2.0—0.3	39,40
Glyceraldehyde 3-phosphate	4.2—4.4	39
Fructose 1,6-diphosphate(1P)	4.0—4.4	39
Fructose 1,6-diphosphate(6P)	3.8—4.0	39
Fructose 6-phosphate	2.6—4.1	39
2,3-Diphosphoglycerate(2P)	2.6	39
2,3-Diphosphoglycerate(3P)	3.3	39
Glycerol 2-phosphate	4.1	39
Glycerol 1-phosphate	4.4	39
Glucose 1-phosphate	2.6	39
Phosphoethanolamine	3.4—3.7	39,40
Phosphorylcholine	3.1	39
Phosphoglycolate	3.2	40
AMP	3.7—4.0	39
Phosphoramidates		
Phosphoarginine	— 3.0—(— 3.5)	6,39
N <sup>ε</sup> -Phospholysine	3.2	40
N(π) Phosphohistidine	— 5.5	8
N(τ) Phosphohistidine	— 4.5	8,42
Phosphocreatine	— 2.3—(— 2.5)	6,39
Acyl phosphates		
β-Phosphoaspartate	— 11.6	43
Acetyl phosphate	— 1.5—(— 2.3)	6,40
Carbamyl phosphate	— 1.1—(— 1.8)	6,40
Cyclic phosphates		
2',3'-cCMP	20.3	44
3',5'-cUMP	— 2.6	44
Phosphodiester		
DNA, RNA	0—1	39
Phospholipids	0—(— 1)	39
Serine ethanolamine phosphate	— 0.4	39
sn-Glycerol 3-phosphoryl-choline	— 0.1	39
sn-Glycerol 3-phosphoryl-serine and ethanolamine	0.4	39
Diphosphodiester		
FAD	— 10.8, — 11.3	19
NAD and NADH	— 10.5, — 11.3	39
UDP-Glucose	— 10.3, — 12.0	45
Diphosphoester		
ADP α-P	— 10.3—(— 10.4)	39

**Table 2 (continued)**  
**<sup>31</sup>P CHEMICAL SHIFTS OF SOME BIOLOGICAL COMPOUNDS**  
**AT ABOUT pH 7<sup>a</sup>**

Compound	Chemical shift <sup>a</sup> (ppm)	Ref.
ADP β-P	-6.1—(-7.4)	39
Triphosphoesters		
ATP α-P	-10.4—(-10.8)	39
ATP β-P	-21.2—(-21.4)	39
ATP γ-P	-5.7—(-6.7)	39

- <sup>a</sup> The chemical shift will change as functional groups are titrated, e.g., lowering pH to protonate phospho groups causes an upfield change in chemical shift of 3.5 to 4 ppm for phosphomonoesters, 2.5 ppm for phosphoramidates, and 5 ppm for acyl phosphates.  
<sup>b</sup> Shifts are reported relative to external 85% H<sub>3</sub>PO<sub>4</sub>. Downfield peaks are positive.

**Table 3**  
**pH DEPENDENCE OF THE <sup>31</sup>P CHEMICAL SHIFTS OF**  
**PHOSPHORYL DERIVATIVES OF THE TETRAPEPTIDE GLY-**  
**GLY-HIS-ALA<sup>a</sup>**

NMR signal <sup>b</sup>	pK <sub>1</sub>	pK <sub>2</sub>	δ <sub>1</sub> (ppm)	δ <sub>2</sub> (ppm)	δ <sub>3</sub> (ppm)
[ <i>P</i> -gly-gly-his-ala]	1.7	7.2	-11.2	5.64	7.94
[ <i>P</i> -gly-gly-(3 <i>P</i> -his)-ala]	1.8	7.3	-6.8	5.45	7.95
[gly-gly-(1,3 <i>P</i> <sub>2</sub> -his)-ala]	2.4	9.1	-11.6	-4.48	-4.42
[gly-gly-(1,3 <i>P</i> <sub>2</sub> -his)-ala]	2.4	8.7	-9.4	-5.20	-4.96
[ <i>P</i> -gly-gly-(3 <i>P</i> -his)-ala]	2.8	7.8	-10.3	-4.50	-4.81
[gly-gly-(3 <i>P</i> -his)-ala]	2.3	7.3	-9.5	-4.63	-4.82
[gly-gly-(1 <i>P</i> -his)-ala]	2.0	8.0	-10.5	-5.04	-5.46

- <sup>a</sup> The pK values and the chemical shifts δ<sub>1</sub>, δ<sub>2</sub>, and δ<sub>3</sub> of the variously protonated species were determined by a nonlinear least squares fit of the experimental chemical shift at a particular pH, δ<sub>exp</sub>, by the equation:

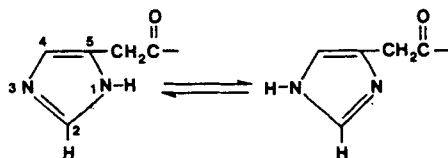
$$\delta_{\text{exp}} = \delta_1 + \sum_{i=1}^n (\delta_{i+1} - \delta_i) \frac{10^{(\text{pH} - \text{pK}_i)}}{1 + 10^{(\text{pH} - \text{pK}_i)}}$$

- <sup>b</sup> The observed phosphoryl group is in italics.

From Kalbitzer, H. R. and Rösch, P., *Org. Magn. Reson.*, 17, 88, 1981. With permission.

spectra of some tetrapeptides containing phosphohistidines. It was shown that the site of phosphorylation, the N(π) or N(τ) position of histidine as well as the N-terminus, could be determined from the NMR spectra. The pH dependence of the <sup>31</sup>P resonance of a series of phosphorylated tetrapeptides is given in Table 3. The chemical shifts for *phosphoryl groups on the N-terminus* can be clearly distinguished from those of phosphohistidines. Phosphorylation of ala-ala-ala-ala also produces a resonance at 6.3 ppm, but the *N*-acetylated Ac-ala-ala-ala-ala does not yield a phosphoryl derivative.<sup>47</sup> The <sup>31</sup>P resonances for the N-terminal phosphoryl groups exhibit spin-spin splitting with a coupling constant of 10.5 Hz, the ala tetrapeptide yielding a doublet (from the lone C-α proton), and the gly tetrapeptides yielding triplets (from the two C-α protons). The chemical shifts for the N-terminal phosphoryl groups are downfield compared with the other phosphoramidates (cf., Table 2), but they shift the same 2.5 ppm upfield upon protonation.

The chemical shifts of the phosphohistidines are rather distinguishing in comparison with other phosphorylated amino acid residues, as seen from Tables 2 and 3. Furthermore, phosphorylation at the N( $\pi$ ) or N( $\tau$ )



position can be distinguished by: (1) the  $^{31}\text{P}$  resonance from the N( $\pi$ ) phosphohistidine residue being further upfield; (2) larger change in the  $^{31}\text{P}$  chemical shift for the N( $\pi$ ) phospho-derivative ( $\sim 0.4$  vs.  $0.2$  ppm) upon protonation; (3) a larger increase in the pK value upon phosphorylation for the N( $\pi$ )phospho-derivative ( $1$  vs.  $0.2$  pH units); and (4)  $^1\text{H}$  NMR.<sup>47</sup> Before using such criteria with a phosphoprotein, one must be assured that the sample is in the random coil state.

As seen in Table 2, the  $^{31}\text{P}$  chemical shift of  $\beta$ -phosphoaspartate is found far upfield of the other phospho-amino acids. In fact, the chemical shift of the phosphoaspartate residue formed upon double phosphorylation of the dipeptide ser-asp was observed even further upfield at  $-17.4$  ppm.<sup>43</sup> The resonance was a poorly resolved triplet due to coupling with the methylene protons. It is apparent that acetyl phosphate with a  $^{31}\text{P}$  resonance at  $-2$  ppm is not a good model.

#### IV. NMR STUDIES OF PHOSPHOPROTEINS

As discussed elsewhere in this volume, protein phosphorylation (usually via ATP) and dephosphorylation play an important role in regulation. In addition, enzyme-catalyzed phosphoryl transfer reactions often entail covalently phosphorylated enzyme intermediates in the mechanism of the reaction. On occasion, the phosphorylated enzyme intermediate (E-P) can be present in sufficient amounts for  $^{31}\text{P}$  NMR studies. Some examples of these will be discussed shortly. However, in many cases, the covalent E-P intermediate is too unstable to examine directly. One can still use  $^{31}\text{P}$  NMR, analyzing substrates and products, to infer information about E-P intermediates. Some of this has been reviewed by Cohn and Rao,<sup>1</sup> and the use of the  $^{17}\text{O}$  and  $^{18}\text{O}$  isotopic effects on  $^{31}\text{P}$  NMR spectra, in some cases, to elucidate E-P intermediates, has been reviewed by Cohn.<sup>22</sup>

There are some instances where phosphorus-containing B vitamins in their role as coenzymes become covalently attached to enzymes. (Note: the  $^{31}\text{P}$  chemical shifts of some of these coenzymes are listed in Table 2.)  $^{31}\text{P}$  NMR studies of these covalently bound coenzymes have not been carried out, but a  $^1\text{H}$  NMR study did identify details in the linkage of the prosthetic group of citrate lyase via a phosphodiester bridge to a serine residue.<sup>48</sup>

As one will note from the discussion on  $^{31}\text{P}$  NMR spectra of amino acids and peptides in the preceding section, the NMR spectral parameters can be used in large measure to identify the phosphorylation site in phosphoproteins which contain phospho-amino acid residues. The *caveat* in this approach is that the protein must be denatured such that a soluble, random-coil form of the phosphoprotein is studied. As discussed at some length previously,<sup>3</sup> the effects of tertiary structure in proteins can modify chemical shifts significantly. In particular, Porubcan et al.<sup>9</sup> have observed that formation of salt bridges, notably involving a histidyl residue and glutamyl or aspartyl residues, can alter  $^{31}\text{P}$  spectral parameters. As an example, we note that binding of  $\text{Mg}(\text{II})$  to ATP causes a downfield shift of about  $0.5$ ,  $1$ , and  $3$  ppm for the  $\alpha$ -,  $\beta$ -, and  $\gamma$ -phosphoryl resonances, respectively. Binding of paramagnetic metal ions could have even more profound effects (cf. Section II.B.1).



If possible, catalytic cleavage and study of the resultant phosphopeptide may be rewarding in that the line width of the peptide (in comparison with the larger protein, cf. Section II.B.2) may be sufficiently narrow that the presence or absence of spin-spin splitting in the phosphorus resonance may be ascertained, thus aiding in identification.

Confirmation of the identification may be made by chemical means. Sometimes, the  $^{31}\text{P}$  NMR spectrum can be monitored as chemical manipulation is performed. One must be aware of the possibility of phosphoryl group migration with some chemical analysis methods, however. Although the chemical treatments are covered in detail elsewhere, we may summarize by noting that (1) phosphoesters are acid stable and base labile; (2) phosphoramidates are base stable and acid labile, and acyl phosphates are subject to cleavage by both acid and base as well as hydroxylamine.

Some of the  $^{31}\text{P}$  NMR studies of phosphoproteins are briefly discussed below. The phosphoproteins are grouped according to the type of phosphoryl residue with further subdivisions for the apparent role of the residue: as a polyelectrolyte with many phosphoamino acid residues, either as an active or structural aid to enzyme catalysis, or as a means of regulating protein function.

### A. Phosphomonoesters

It appears that all phosphomonoester-containing proteins studied by  $^{31}\text{P}$  NMR to date contain phosphoserine rather than phosphothreonine residues.

#### 1. Polyelectrolytes

Some proteins contain several serine residues, many of which are phosphorylated. The effect of this multiple phosphorylation is to create a polyanion which can bind metal ions.

##### a. Casein

The first example of identification of phosphorylation sites on phosphoproteins was provided by the investigation of Ho et al.<sup>46</sup> on bovine  $\alpha_1$ -casein B (mol wt 27,300), one of the half dozen or so caseins aggregated in milk. The spin-spin splitting (triplet), chemical shift, and pH dependence of the chemical shift of the phosphorus resonance of  $\alpha$ -casein in 8 M urea solution all led to the conclusion that the several phosphorylated residues were phosphoserines. This conclusion was reached on the basis of comparison with those parameters for model compounds, including the amino acid phosphoserine.

Recently, two other studies of the  $^{31}\text{P}$  spectra of caseins have been reported. In both instances, some care was taken to remove paramagnetic ions which can cause line broadening. With this precaution, the  $^{31}\text{P}$  spectra of the caseins yielded resolved resonance lines.<sup>49,50</sup> The  $^{31}\text{P}$  spectrum of  $\alpha_1$ -casein B (spectrum A) and the 62-amino-acid peptide formed by cyanogen bromide treatment (spectrum B) are shown in Figure 3. As anticipated, the smaller peptide has narrower line widths. The  $^{31}\text{P}$  spectra of  $\beta$ -casein A<sub>2</sub> (spectrum A) and the  $\beta$ 1-25 tryptic peptide (spectrum B) are displayed in Figure 4. The spectra are interestingly diverse in spite of the similarity of the caseins. Quite obviously, the local environment strongly influences chemical shifts of the phosphoserine residues.

Sleigh et al.<sup>49</sup> assigned the phosphorus peaks by comparison of the spectra obtained from the two caseins and the various peptide fragments. Peak e in Figure 4 was assigned to phosphoserine-35 and the overlapping peaks labeled a, b, and c were assigned (not necessarily in order) to the cluster phosphoserines of  $\beta$ -casein, i.e., to those at positions 15, 17, 18, and 19. In their study of  $\beta$ -casein, Humphrey and Jolley<sup>50</sup> monitored the pH dependence of the  $^{31}\text{P}$  resonances of the phosphoprotein as well as the  $\beta$ 1-25 tryptic peptide. It was concluded that the ionization was influenced by neighboring residues. This led to further assignments of overlapping a, b, and c peaks in Figure 4, with the resonances to lower field decreasing in the order phosphoserine 18 > 17, 19 > 15.

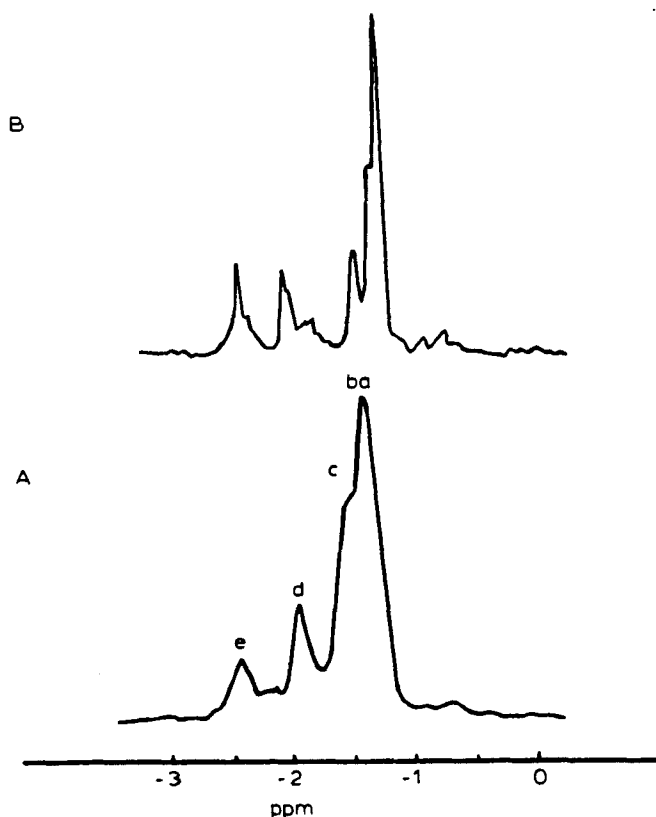


FIGURE 3. Proton-decoupled  $^{31}\text{P}$  NMR spectra (40.5 MHz) of (A)  $\alpha_{s1}$ -casein B and (B) the 62-amino-acid peptide isolated after cyanogen bromide cleavage. The buffer is 0.1 M KCl, 20 mM Pipes, 2 mM EDTA, pH 6.8, 10%  $\text{D}_2\text{O}$ . (From Sleight, R. W., MacKinlay, A. G., and Pope, J. M., *Biochim. Biophys. Acta*, 742, 175, 1983. With permission.)

Humphrey and Jolley<sup>50</sup> also measured the spin-lattice and spin-spin relaxation times of  $\beta$ -casein and its phosphopeptide. They concluded that there was little or no restriction in the segmental motion in the region of the phosphoserine cluster.

### **b. Phosvitin**

Phosvitin (mol wt 35,000) from hen egg yolk is largely composed of serine, 120 of the 220 amino acid residues. And most of the serine residues (112) are phosphorylated. In their early investigation, Ho et al.<sup>46</sup> used  $^{31}\text{P}$  NMR to demonstrate that the serines were phosphorylated. More recent studies have found that the phosphorus environments exhibit some heterogeneity as manifest in the multiple peaks observed in the  $^{31}\text{P}$  NMR spectrum.<sup>49,51</sup> Although the  $\text{pK}_a$  (5.8) determined by monitoring the  $^{31}\text{P}$  resonances as a function of pH was typical of phosphoserine for most of the phosvitin phosphoserines, the titration curves revealed negative cooperativity, suggesting interactions between the different phosphoserines, which occur in clusters on the protein.<sup>51</sup> The proton NMR results further indicated that positively charged histidine residues interacted with some of the phosphoserine residues.<sup>51</sup>

$^{31}\text{P}$  NMR experiments have also been carried out with the crystalline complex of lipovitellin with phosvitin since the complex occurs in egg yolk.<sup>35</sup> The complex, obtained from *Xenopus*, contained almost 100 mol of bound phospholipid for each phosvitin. Separate, well-resolved resonances were seen for the phosphorus nuclei of the phospholipid (phosphodiester) and

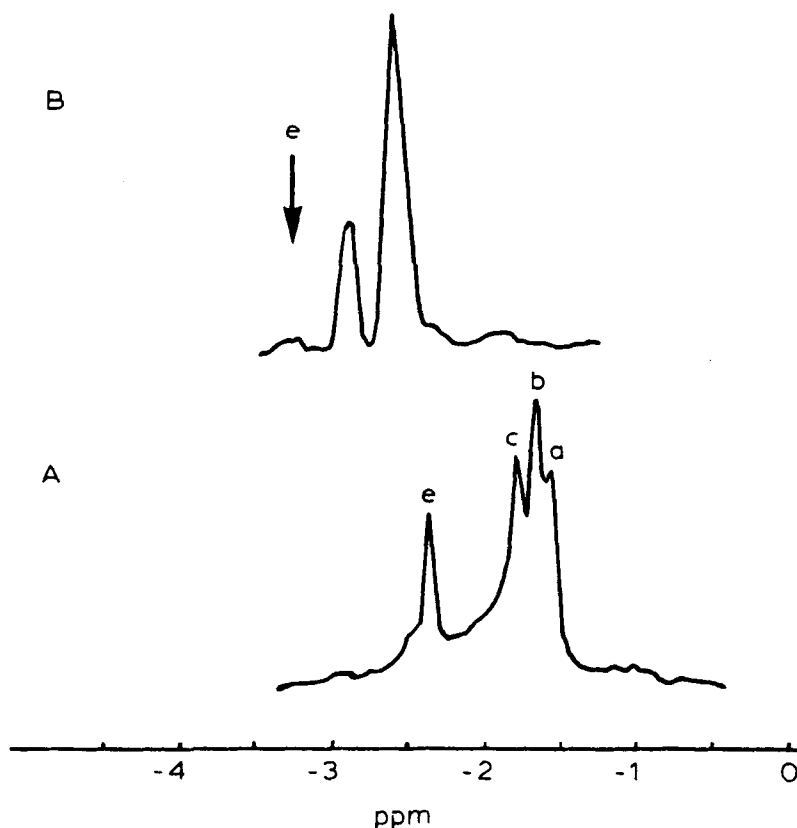


FIGURE 4. Proton-decoupled  $^{31}\text{P}$  NMR spectra (40.5 MHz) of (A)  $\beta$ -casein  $\text{A}_2$  and (B) the  $\beta$ 1-25 peptide isolated after trypsin digestion. The buffer is listed in Figure 3. (From Sleight, R. W., MacKinlay, A. G., and Pope, J. M., *Biochim. Biophys. Acta*, 742, 175, 1983. With permission.)

phosvitin (phosphomonoester).<sup>35</sup> Spin-lattice relaxation time measurements revealed that the phosphoserines possess much faster reorientation rates than the phospholipids.

#### **c. Rat-Incisor-Dentine Phosphoprotein**

Rat incisor dentine contains a phosphoprotein which consists of about 90% serine and aspartate, with 87% of the serines phosphorylated.<sup>52</sup> A pH titration of the  $^{31}\text{P}$  resonance had a midpoint of 7.2, but the cooperativity apparent from the titration curve suggested that an extensive hydrogen-bonding network occurred along the highly charged polyanionic surface of the phosphoprotein.<sup>53</sup> EPR and proton NMR experiments using  $\text{Mn(II)}$  as a paramagnetic probe demonstrated the efficacy of the polyanion for metal ion binding.<sup>53</sup>

#### **d. Saliva Phosphoproteins**

Among other techniques, Bennick et al.<sup>54</sup> employed  $^{31}\text{P}$  NMR in their studies of the proline-rich phosphoproteins from saliva. The phosphoprotein contains a couple phosphoserine residues which apparently play a role in calcium binding. Addition of calcium chloride results in the  $\text{pK}_a$  being decreased from 6.5 to 5.9 for each phosphoserine residue. In addition, alkaline phosphatase cleavage of the phosphoryl groups diminished the calcium binding affinity of the protein.

## 2. Enzyme Catalysis

As mentioned earlier, some phosphoenzyme intermediates have been isolated, and  $^{31}\text{P}$  NMR offers a means of elucidating certain aspects of the enzyme mechanism.

### a. Alkaline Phosphatase

The most widely studied phosphoprotein investigated by NMR is *E. coli* alkaline phosphatase (mol wt 94,000), a dimeric zinc metalloenzyme which catalyzes the nonspecific hydrolysis of phosphomonoesters. The enzyme has been subjected to analysis via  $^1\text{H}$ ,  $^{13}\text{C}$ ,  $^{31}\text{P}$ , and  $^{113}\text{Cd}$  NMR, the latter by virtue of the fact that the enzyme retains some activity when the  $\text{Zn(II)}$  is substituted by  $\text{Mn(II)}$ ,  $\text{Co(II)}$ ,  $\text{Cu(II)}$ , or  $\text{Cd(II)}$ . Several  $^{31}\text{P}$  NMR studies have shown that covalent (E-P) and noncovalent (E·P) enzyme intermediates exist in the catalytic mechanism of native alkaline phosphatase; the E-P intermediate (8.6 ppm) and E·P intermediate (4.2 ppm) can easily be distinguished from one another as well as the product, inorganic phosphate (2 ppm).<sup>40,55-62</sup> The intermediate E-P has phosphorylated ser-102 at the active site, since the resonance for the E-P intermediate is considerably downfield from that usually found for phosphoserine. Bock and Sheard<sup>40</sup> and Chlebowski et al.<sup>55</sup> argued that the phosphoserine was experiencing some strain; it will be noted in Table 2 that the strained cyclic nucleotide 2',3'-cCMP resonance is shifted far downfield.

Substitution of  $\text{Mn(II)}$  or  $\text{Co(II)}$  for  $\text{Zn(II)}$  in the metalloenzyme resulted in disappearance of the enzyme-bound phosphoryl signals.<sup>40,55</sup> This was attributed to the resonances being so broad as to be undetectable due to presence of the paramagnetic metal ions near the bound phosphoryl. An upper limit of 3.3 Å for the Co-P distance was estimated.<sup>40</sup>

The relative proportions of the E-P and E·P intermediates in the three-stage equilibrium  $\text{E} + \text{P}_i \rightleftharpoons \text{E} \cdot \text{P} \rightleftharpoons \text{E-P}$  depend on pH and the metal ion composition of the enzyme. For the native zinc enzyme, the E-P and E·P resonances trade intensity as the pH is varied, the covalent E-P intermediate completely dominating at pH < 5 and the noncovalent E·P intermediate completely dominating at pH > 6.4. Substitution of  $\text{Cd(II)}$  for  $\text{Zn(II)}$  results in an enzyme with <1% of the activity, but the E-P resonance has the same chemical shift and is stable to much higher pH values (>7).<sup>40,55</sup> But the E·P phosphorus in the cadmium enzyme resonates at 13 ppm, whereas it resonates at 4 ppm in the zinc enzyme.<sup>59</sup>

The stability of the cadmium enzyme has been one factor in its further study. Another incentive for use of the cadmium enzyme is that the  $^{111}\text{Cd}$  and  $^{113}\text{Cd}$  isotopes, which have nuclear spin  $I = 1/2$ , can be employed.  $^{113}\text{Cd}$  NMR experiments have been performed, but the  $^{113}\text{Cd}$  and  $^{111}\text{Cd}$  can also directly influence the  $^{31}\text{P}$  spectrum as demonstrated by Otvos et al.<sup>59</sup> It was found that the  $^{31}\text{P}$  resonance of E·P, but not the covalent E-P, was split into a doublet  $J \approx 30$  Hz from spin-spin splitting of  $^{113}\text{Cd}$ , thus proving that the phosphate and  $\text{Cd(II)}$  are directly bound in the noncovalent E·P complex. This observation may explain the large effect of metal ion substitution on the E·P chemical shift.

Two tightly bound metal ions are the putative catalytic metal ions. But up to six metal ions can be bound to the enzyme with enhanced activation occurring. Some of the NMR studies have been concerned with the metal ion composition and the stoichiometry of phosphate binding.<sup>57,58,60</sup> Studies subsequent to those of Otvos et al.<sup>59</sup> have focused on the pH dependence of the equilibria between E-P, E·P, and  $\text{P}_i$ . Figure 5 displays the pH dependence of the  $^{31}\text{P}$  spectrum of the  $[\text{^{113}Cd(II)}]_6$ -alkaline phosphatase species with added phosphate, and Figure 6 shows the equilibrium concentrations of the phosphorus species for the zinc and cadmium enzymes as a function of pH. The splitting due to coupling of the  $^{31}\text{P}$  to  $^{113}\text{Cd}$  is evident for the E·P resonance in Figure 5.

The saturation transfer technique was used to obtain rate constants for interconversion of the three phosphorus species E-P, E·P, and  $\text{P}_i$ .<sup>59</sup> The results were in good agreement with values obtained by other methods.

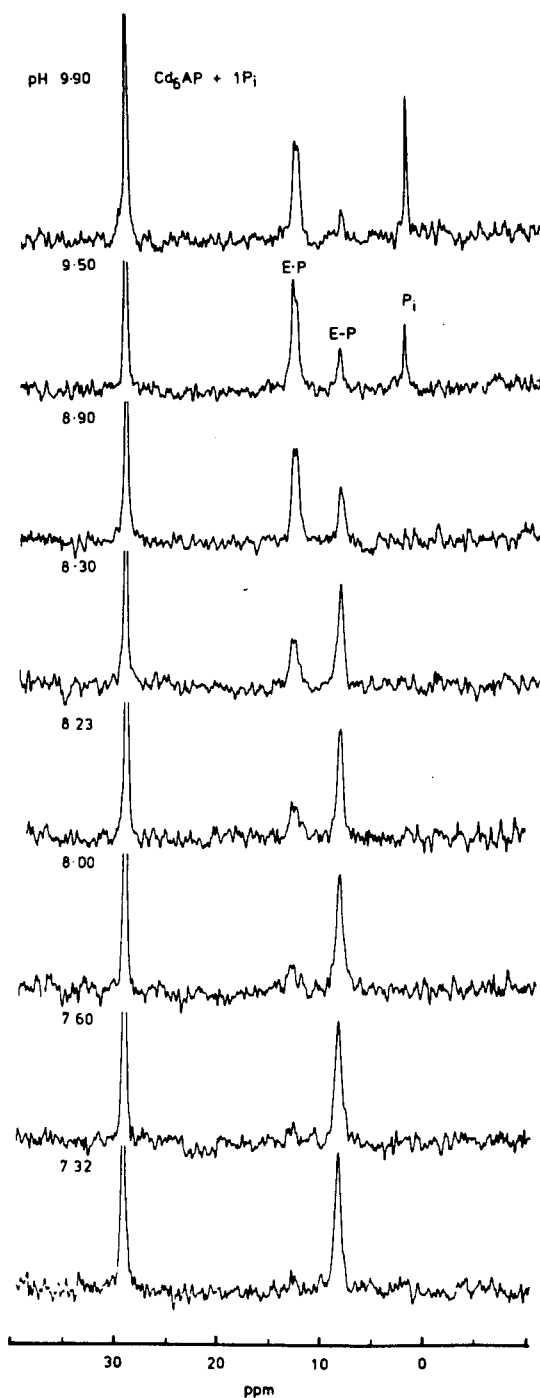


FIGURE 5.  $^{31}\text{P}$  NMR spectra (80.9 MHz) of  $[^{113}\text{Cd}(\text{II})]_6$ -alkaline phosphatase, containing one equivalent of phosphate, as a function of pH. The solution contained 2.0 mM enzyme. Each spectrum is the result of averaging 1000 free induction decays. The resonance most downfield arises from methyl phosphonate, a secondary external reference. (From Gettins, P. and Coleman, J. E., *J. Biol. Chem.*, 258, 408, 1983. With permission.)

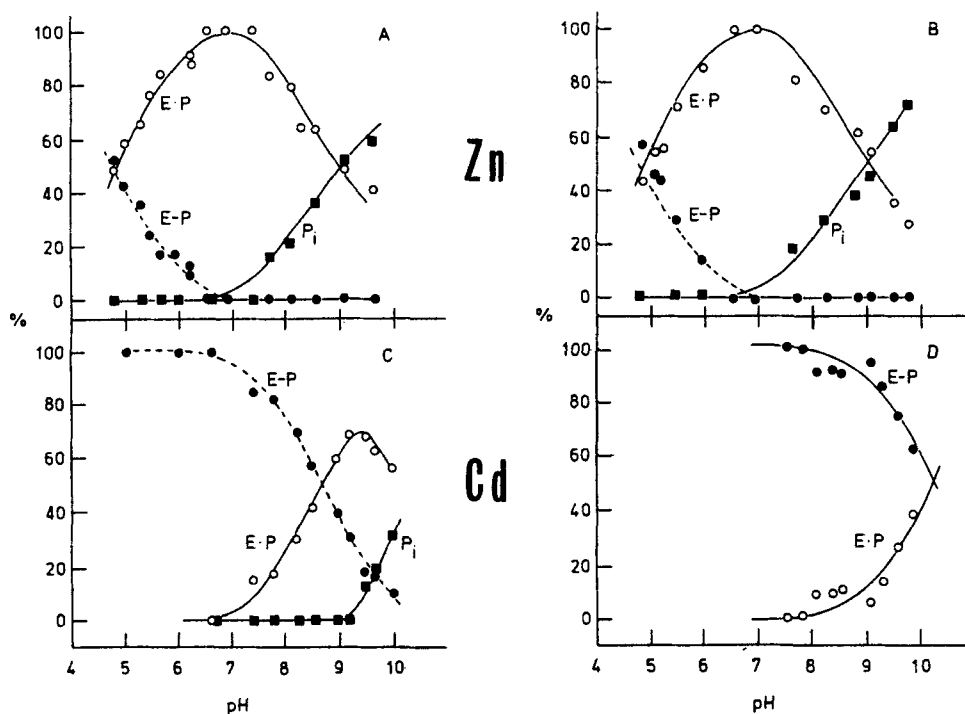


FIGURE 6. Relative equilibrium concentrations of the phosphorus species for zinc- and cadmium-containing alkaline phosphatases (AP) as a function of pH: E-P (●), E-P (○) and  $P_i$  (■). (A) 1.98 mM  $Zn_4AP$  plus one equivalent  $P_i$ ; (B) 2.13 mM  $Zn_4Mg_2AP$  plus one equivalent  $P_i$ ; (C) 2.00 mM  $Cd_4AP$  plus two equivalents  $P_i$ ; (D) 1.83 mM  $Cd_2AP$  plus two equivalents  $P_i$ . Since only one equivalent of phosphate was bound throughout the titration, the percentages of E-P and E-P are normalized to this one equivalent rather than two. (From Gettins, P. and Coleman, J. E., *J. Biol. Chem.*, 258, 408, 1983. With permission.)

### b. Phosphoglucomutase

The phosphorylated form of phosphoglucomutase apparently is an intermediate in the ping-pong mechanism of the enzyme-catalyzed reaction, which entails transfer of a phosphoryl group between glucose-1-phosphate and glucose-6-phosphate. The stability of the phosphoenzyme has enabled  $^{31}P$  NMR studies to be carried out.<sup>23,63</sup> At pD 7.9, the  $^{31}P$  chemical shift was found to be 3.8 ppm and the resonance line width was observed to narrow with proton decoupling.<sup>63</sup> Both points are consistent with a phosphorylated serine residue. Relaxation time measurements ( $T_1$  and line width) were interpreted to mean that the phosphoserine was relatively immobile since the  $T_1/T_2$  ratio yielded a value for the correlation time of  $10^{-7}$  sec, comparable to that for tumbling of the whole protein.<sup>63</sup> (Review Equations 2, 3, and 10 to see how  $\tau_c$  might be obtained from  $T_1/T_2$ .)

Mg(II) activates phosphoglucomutase and has little effect on the  $^{31}P$  chemical shift of the phosphoenzyme. Co(II) and Ni(II) also activate the enzyme. Addition of one equivalent of Co(II) broadened the phosphorus signal beyond detection. Although substantially broadened, the phosphorus signal in the presence of Ni(II) could be observed and relaxation times measured. Using the equations for paramagnetic contributions to nuclear relaxation (Reference 3, Equations 6 to 13), with certain assumptions, a Ni(II)-to-P distance of 4 to 6 Å was calculated.<sup>63</sup> More recent experiments using  $^{113}Cd(II)$  as the activating metal ion discovered the  $^{31}P$  peak split into a doublet due to coupling to  $^{113}Cd(II)$  directly coordinated to the phosphoryl group.<sup>23</sup> The spin-spin splitting was abolished upon addition of substrate, either glucose-1-phosphate or glucose-6-phosphate.<sup>23</sup> It was suggested that the collapsed splitting resulted from rapid motion of the phosphoserine,<sup>23</sup> but it could also be caused by



the  $^{113}\text{Cd}(\text{II})$  no longer being bound directly to the phosphoryl group. However,  $^{31}\text{P}$  NMR experiments with  $^{17}\text{O}$  incorporated into the phosphoryl group on the enzyme also imply that the phosphoserine moiety achieves greater internal mobility upon addition of substrate.<sup>23</sup>

### 3. Regulation of Protein Function

Phosphorylation and dephosphorylation are widely utilized physiological processes which serve to variously activate and inactivate enzymes and other proteins. In general, enzymes involved in synthesis are inactivated by phosphorylation, but those involved in degradative pathways are activated by phosphorylation. Our first case is an example of the latter class.

#### a. Glycogen Phosphorylase a

A conformational change is induced in glycogen phosphorylase resulting in an active enzyme when serine-14 is phosphorylated.<sup>64</sup> This regulatory process is important in maintenance of blood glucose levels and in enabling the energy stored in glycogen to be used for work. Glycogen phosphorylase contains the coenzyme pyridoxal phosphate.  $^{31}\text{P}$  resonances from the coenzyme and the phosphoserine moiety can be resolved.<sup>65</sup>

An investigation of the pH behavior of the phosphoserine resonance found a shift with pH.<sup>6</sup> Analysis of the titration curve led to the suggestion that positively charged groups were interacting with the phosphoserine moiety.

Vogel et al.<sup>6,14</sup> measured the  $^{31}\text{P}$  line width of the phosphoserine residue at four different spectrometer frequencies and concluded that the chemical shift anisotropy (CSA) relaxation mechanism (see Equations 7 and 11) dominated at higher frequencies. Comparing the small dipolar contributions to the line width (see Equations 3 and 11) for the phosphohistidine of succinyl-CoA synthetase (11 Hz) and for the phosphoserine of glycogen phosphorylase (6 Hz), it was concluded that the phosphohistidine residue is in monoanionic form and the phosphoserine residue is in dianionic form at pH 7.25.<sup>14</sup>

On the basis of their  $^{31}\text{P}$  NMR line width studies, Vogel et al.<sup>14</sup> concluded that the phosphoserine residue of glycogen phosphorylase experiences two separate conformations. This is consistent with the earlier observation by Hoerl et al.<sup>66</sup> that the  $^{31}\text{P}$  resonance was split.

#### b. Muscle Proteins

$^{31}\text{P}$  NMR has been used to study many aspects in the mechanism of muscle contraction, most notably interactions with ATP or ADP. However, regulation here too involves protein phosphorylation. *Troponin* together with tropomyosin mediates the calcium dependence of muscle contraction. In response to binding  $\text{Ca}(\text{II})$ , the troponin-tropomyosin complex modifies its interaction with actin filaments such that muscle contraction can occur. A  $^{31}\text{P}$  NMR signal has been observed for troponin which has chemical shift and pH dependence characteristic of phosphoserine. Complexation with tropomyosin did not affect the resonance.<sup>67</sup>

A phosphorus resonance from the phosphoserine in *tropomyosin* shifts with pH.<sup>6</sup> The pH titration curve implies charged groups are near the phosphoserine. The line width indicates a substantial degree of motional freedom.<sup>6</sup>

*Myosin* interaction with actin filaments is the central feature of muscle contraction. According to the  $^{31}\text{P}$  NMR spectra of Koppitz et al.<sup>68</sup> on purified myosin, myosin also possesses a phosphoserine residue. Its characteristics suggest it is on the protein surface.

### 4. Others

#### a. Pepsinogen

Pepsin and pepsinogen contain phosphorus. It is not clear what the functional significance if any, of the phosphorylated amino acid residue is, however.  $^{31}\text{P}$  NMR experiments by Edmondson and James<sup>7</sup> on pepsinogen indicate that a serine residue is phosphorylated,

forming a monoester. This conclusion was based on the  $^{31}\text{P}$  chemical shift and the pH dependence of that chemical shift.

### **b. Ovalbumin**

Although the function of hen egg white ovalbumin is not understood, this glycoprotein, which is also phosphorylated, has been widely studied.  $^{31}\text{P}$  NMR is included in the list of techniques applied to ovalbumin.<sup>49,69</sup> Phosphoserine-68 and -344 yield two well-resolved  $^{31}\text{P}$  resonances with chemical shift and pH dependence behavior typical of phosphoserines. In fact, the pH titration behavior, together with susceptibility to phosphatase cleavage, indicates that the phosphoserines are located at the surface of the native protein.<sup>69</sup> One resonance (5.0 ppm at pH 8.3) was assigned to phosphoserine-344 and was less accessible for phosphatase cleavage, especially at high pH.

The pH titration and the  $^{31}\text{P}$ - $^1\text{H}$  coupling constants of both residues implied that the phosphoserine residues were not interacting with other charged groups in the protein.<sup>69</sup> Analysis of the frequency dependence of the line widths suggested that phosphoserine-344 has a greater degree of mobility than phosphoserine-68.

Addition of magnesium chloride results in upfield shifts of both phosphorus resonances.<sup>69</sup> However, the relatively weak metal ion binding constants suggest that the phosphoryl groups do not participate directly in  $\text{Mg(II)}$  binding.

### **c. Phosphoproteins in Insect Hemolymph Sera**

In recent years there has been a boom in  $^{31}\text{P}$  NMR studies of intact cells, tissues, and whole organisms. Most of these studies have focused on investigating small phosphorus metabolites such as ATP,  $\text{P}_i$ , and phosphocreatine.<sup>39</sup> However, signals from larger phosphorus-containing structures are occasionally observed, usually phospholipids or nucleic acids. Mueller et al.<sup>70</sup> obtained the  $^{31}\text{P}$  NMR spectra of the hemolymph sera from tobacco hornworm. In addition to identifying the resonances from several small phosphorus metabolites, they observed some resonances from macromolecular species. Some of the resonances were too far downfield to be ascribed to nucleic acids or phospholipids. Therefore, it was concluded that they originated from phosphoproteins.

## **B. Phosphoramidates**

Although other amino acid residues can become phosphorylated to form phosphoramidates (see Table 2),  $^{31}\text{P}$  NMR studies of proteins containing phosphoramidates have so far encountered phosphohistidine residues.

### **1. Enzyme Catalysis**

#### **a. Succinyl-CoA Synthetase**

Succinyl-CoA synthetase from *E. coli* is a tetramer with an  $\alpha_2\beta_2$  structure and two active sites at the interface of each  $\alpha$ - and  $\beta$ -subunit. The putative mechanism of catalysis entails a covalent phosphohistidine residue. A  $^{31}\text{P}$  resonance for the enzyme has been observed at  $-4.8$  ppm.<sup>42</sup> By comparison with the chemical shifts listed in Table 2 for  $\text{N}(\pi)$  and  $\text{N}(\tau)$  phosphohistidines, it is clear that this value is consistent with phosphorylation at the  $\text{N}(\tau)$  position of a histidine residue. A comparison of the dipolar contributions to the line width, extracted from the frequency dependence of the line width, for the residues in succinyl-CoA synthetase and glycogen phosphorylase led Vogel et al.<sup>14</sup> to conclude that the  $\text{N}(\tau)$  phosphohistidine on succinyl-CoA synthetase was in the monoanionic form at pH 7.25. From the CSA contributions to the line width, it was deduced that the phosphohistidine moiety is immobile on the enzyme, possessing no motion other than tumbling of the protein itself.

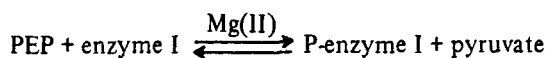
A divalent cation is needed to activate the enzyme. The natural activator  $\text{Mg(II)}$  results in an upfield shift of the phosphorus resonance.<sup>42</sup> From the titration curve of the resonance

with addition of Mg(II), a dissociation constant of 4 mM was obtained in reasonable agreement with the value of 10 mM required for maximal activity of the enzyme. Mn(II) will also activate succinyl-CoA synthetase. Use of Mn(II) broadened the phosphorus resonance beyond detection, leading to the conclusion that Mn(II) is bound within 10 Å of the phosphorylation site and to the suggestion that the Mn(II) interacts with the phosphohistidine.<sup>42</sup> That suggestion is not necessarily in accord with the observation that Mn(II) binds with equal affinity to the phosphorylated and dephosphorylated enzyme.<sup>71</sup>

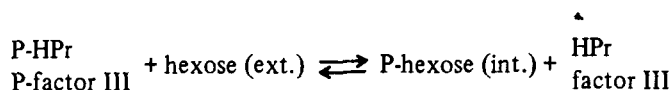
Addition of the substrate CoA, with or without Mg(II) present, resulted in substantial line broadening and downfield shifts.<sup>42</sup> It was suggested that this line broadening may arise from exchange between two enzyme conformations with CoA bound. Addition of the competitive inhibitor 2,2'-difluorosuccinate sharpened the resonance and shifted it back upfield, thus implying that the phosphoryl residue was locked into a single conformation. On the basis of their observations, Vogel and Bridger<sup>42</sup> proposed a detailed mechanism for the enzymic catalysis.

### **b. Phosphoenolpyruvate-Dependent Phosphotransferase System**

Phosphoenolpyruvate (PEP) is used as the energy source for sugar uptake and phosphorylation in several bacteria. The phosphotransferase system evidently consists of four enzymic reactions entailing phosphoenzyme intermediates:



and, depending on the system,



where HPr is a small (mol wt 7685) heat-stable protein.

HPr isolated from *Staphylococcus aureus* has been studied by Gassner et al.,<sup>8</sup> and HPr isolated from *E. coli* has been studied by Dooijewaard et al.<sup>72</sup> Both investigations utilized <sup>31</sup>P and <sup>1</sup>H NMR. For both species a resonance at -4.1 ppm was observed in the presence of excess PEP and catalytic amounts of enzyme I. The -4.1 ppm resonance is clearly distinguished from that of PEP or P<sub>i</sub> (see Table 2) and can be attributed to the phosphohistidine residue on HPr. The chemical shift changed to -5.4 ppm when the enzyme was subjected to irreversible alkaline denaturation (pH 12.8) followed by near neutralization of the pH. That chemical shift value indicates that the phosphorylation occurs at the N(π) position of the histidine (see Table 2). It is interesting that reaction of HPr with phosphoramidate results in phosphorylation at the N(τ) position of the histidine, yielding an inactive phosphorylated HPr.<sup>8</sup> Titrations following the phosphorus resonance and the histidine proton resonance yielded identical pK<sub>a</sub> values of 7.8. Thus, a two-unit increase in pH from the value of pK<sub>a</sub> = 5.6 results from the phosphorylation.<sup>71</sup> This increase in pK<sub>a</sub> is larger than usual due to phosphorylation of a histidine at N(τ) (see discussion in Section III). Based on line width considerations, it was concluded that the phosphohistidine was immobilized on the protein.<sup>14</sup>

It may be noted that purification of other components in the PEP-dependent phosphotransferase system has been accomplished. <sup>1</sup>H NMR studies have been carried out to elucidate the phosphohistidine moiety of factor III.<sup>73</sup>

## 2. Histones

Histones are small proteins with a large amount of positively charged amino acids (arginine and lysine). The positive charges enable the histones to bind tightly to DNA, thus folding the DNA into the nucleosome moiety of chromosomes. Phosphorylation of histones has been implicated in causing the chromosome condensation during cell mitosis. Although phosphorylation of serines has been largely linked to this event, it appears that histidine phosphorylation may also play a regulatory role.

Fujitaki et al.<sup>74</sup> have utilized <sup>31</sup>P NMR in an investigation of enzymatically and chemically phosphorylated histone H4 (mol wt 11,000). Histone H4 phosphorylated by kinase from regenerating rat liver exhibits a resonance at -5.4 ppm upon denaturation; this implies protonation at the N3 position of a histidine residue. But when H4 is phosphorylated by kinase in nuclei of Walker-256 carcinosarcoma, the denatured protein yields a resonance at -4.9 ppm, characteristic of histidine N-1 phosphorylation. In confirmation, it was found that the phospho-residues were acid labile. Chemical phosphorylation by treatment with phosphoramidate gave acid-labile phospho-amino acid residues on H4. The <sup>31</sup>P spectrum of the structural protein revealed a narrow peak at -4.8 ppm and a broad peak at -7.3 ppm. It was concluded that both his-18 and his-75 were phosphorylated at the N(τ) position. Peptide fragments H4(1-23) and H4(38-102) yield single resonances in accord with that conclusion.

## C. Acyl Phosphates — Adenosinetriphosphatase

Adenosinetriphosphatases (ATPase) which catalyze the ATP hydrolysis providing the energy necessary for active transport of cations apparently become phosphorylated intermediates during the hydrolytic process. These membrane-bound transport ATPases can be solubilized with detergents (e.g., sodium dodecyl sulfate).

Fossel et al.<sup>43</sup> have examined the <sup>31</sup>P NMR spectra of sodium- and potassium-activated ATPase [(Na,K)ATPase] from the salt gland of the duck following addition of ATP to the enzyme in the presence of Mg(II) and Na<sup>+</sup>. Previous research has indicated that an aspartyl residue becomes phosphorylated under these circumstances. Quite surprisingly, they observed a resonance at -17 ppm. This is about 15 ppm upfield of the resonance position for acetyl phosphate, hitherto considered a decent model compound for acyl phosphate residues on phosphoproteins. Consequently, Fossel et al.<sup>43</sup> synthesized two other model compounds and obtained <sup>31</sup>P spectra. The spectrum of purified β-phosphoaspartate yielded a peak at -11.6 ppm. The spectrum of the unpurified reaction mixture obtained with phosphorylation of L-seryl-L-aspartate yielded a peak at 3.7 ppm (characteristic of phosphoserine) and one at -17.4 ppm which, most reasonably, was attributed to a phosphoryl group attached to the aspartyl residue.

Fossel et al.<sup>43</sup> also examined the <sup>31</sup>P resonance of calcium-activated ATPase obtained from sarcoplasmic reticulum. It also had a resonance at -17.5 ppm. As hydroxylamine is known to cleave acyl phosphates, the enzyme was treated with hydroxylamine, resulting in loss of the -17.5 ppm peak. Addition of potassium ion, which destabilizes the intermediate, also results in loss of the resonance.

The difference in phospho-amino acid chemical shifts obtained for the ATPase and the monomeric phospho-amino acid is the largest of any phosphoprotein yet reported, an even larger difference than that of alkaline phosphatase. Incidentally, it should be noted that acetyl phosphate appears to be a poor model compound.

## D. Disubstituted Phosphorus Residues

Previous investigation on pepsin and pepsinogen suggested that the phosphorus on the enzyme was present in a phosphodiester linkage.<sup>75</sup> Subsequent dephosphorylation experiments, however, demonstrated that the phosphorus-containing group was a phosphomonoester.<sup>76</sup> As mentioned in Section IV.A.4.a, <sup>31</sup>P NMR experiments confirmed that conclu-

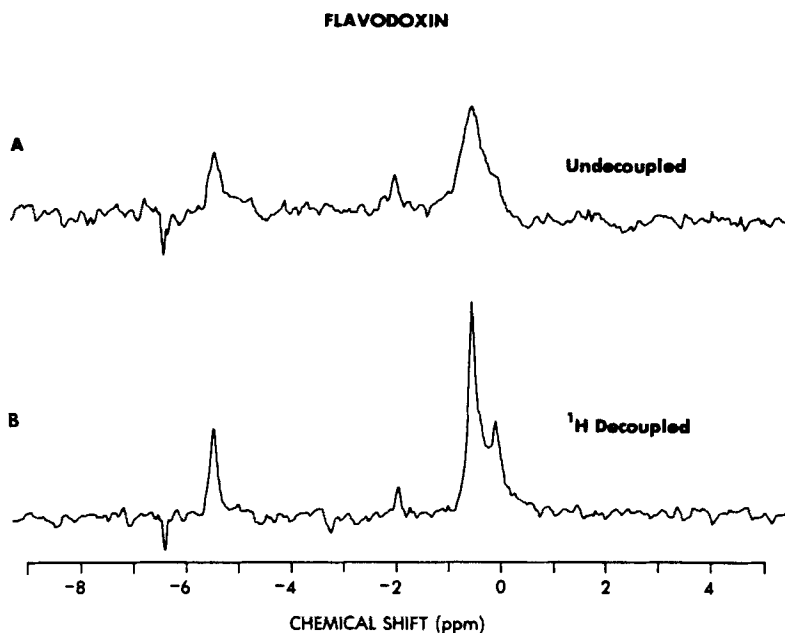


FIGURE 7.  $^{31}\text{P}$  NMR spectra (40.5 MHz) of native *Azotobacter* flavodoxin (oxidized form) in 100 mM Tris buffer, pH 8.0. (A) Spectrum without proton decoupling; (B) spectrum with broadband proton decoupling. The small peak at 2.0 ppm probably arises from  $\text{P}_i$  and was not present in most spectra. (From Edmondson, D. E. and James, T. L., *Proc. Natl. Acad. Sci. U.S.A.*, 76, 3786, 1979. With permission.)

sion.<sup>7</sup> Since then, it has been a widely held belief that all phospho-amino acids in phosphoproteins are monosubstituted. However, recent work on two phosphoproteins has indicated that phospho bridges between amino acid residues on the same polypeptide strand may exist. These will be discussed below.

### 1. *Azotobacter* Flavodoxin

Low-potential electron-transfer flavoproteins called flavodoxins are found in several bacteria and algae. There are two broad classes of flavodoxins, one with molecular weight on the order of 15,000 and one with molecular weight on the order of 23,000. The smaller-sized flavodoxins have been extensively studied by X-ray crystallography among other techniques. The smaller flavodoxins evidently do not contain any phosphorus in addition to that on the flavin mononucleotide (FMN) coenzyme.<sup>7</sup> However, flavodoxin from *Azotobacter vinelandii*, which is representative of the larger flavodoxins, was discovered by Edmondson and James<sup>7</sup> with  $^{31}\text{P}$  NMR to be a phosphoprotein.

The NMR spectra are shown in Figure 7 for *Azotobacter* flavodoxin at pH 8.0. Three peaks, at 5.6, 0.8, and 0.2 ppm, are evident, yet the FMN coenzyme contains a single phosphorus. Chemical analysis confirmed 3 mol of phosphorus per mole of flavodoxin. Various techniques of isolating the protein from *Azotobacter* yielded the same results regardless of whether Tris or phosphate buffers were utilized. Titration of the native protein in the pH range 5.5 to 9.5 produced little or no change in the spectrum. The resonance at 0.2 ppm was gone when flavodoxin aged for 3 to 4 months was passed over a Sephadex G-25<sup>®</sup> column, the other peaks remaining as before.

The FMN, yielding the peak at 5.6 ppm, could be removed by precipitation of the protein with trichloroacetic acid. This treatment also removed the residue producing the 0.2 ppm; but when the apoprotein was maintained in a denaturing medium of 8 M urea, it still gave

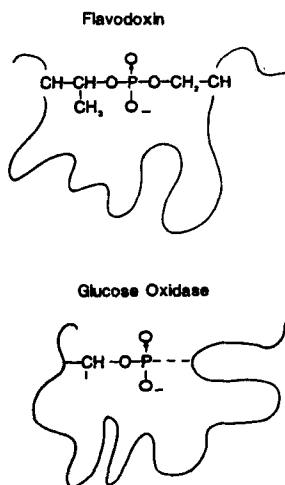


FIGURE 8. Phospho bridges spanning the same polypeptide chain in the protein. Top: flavodoxin. Bottom: glucose oxidase.

a peak at 0.9 ppm. Most interesting was the observation that the peak did not shift with change in pH, thus suggesting its identity as a phosphodiester. Although phosphohistidines also do not titrate ( $<0.4$  ppm), such a phosphoramidate should be cleaved by the acid treatment. Furthermore, the chemical shift is most appropriate for a phosphodiester (see Table 2), and the line narrowing upon proton decoupling which is demonstrated in Figure 7 is in accord with a phosphodiester but not with a phosphohistidine. We note that chemical tests indicated the phosphorus residue was not in a phospholipid or carbohydrate. Subsequent chemical degradation studies confirmed the existence of the intrastrand phosphodiester bridge in *Azotobacter* flavodoxin and identified the participating amino acid residues as a serine and a threonine.<sup>77</sup> This intrastrand phospho bridge is illustrated in Figure 8.

The acid-labile non-FMN residue giving rise to the peak at 0.2 ppm has not been identified, but it was suggested to be in an acyl phosphate linkage with a carboxyl group on the protein based on its susceptibility to cleavage by acid or by hydroxylamine.<sup>77</sup>

the existence of the intrastrand phosphodiester bridge in *Azotobacter* flavodoxin and identified the participating amino acid residues as a serine and a threonine.<sup>77</sup> This intrastrand phospho bridge is illustrated in Figure 8.

The acid-labile non-FMN residue giving use to the peak at 0.2 ppm has not been identified, but it was suggested to be in an acyl phosphate linkage with a carboxyl group on the protein based on its susceptibility to cleavage by acid or by hydroxylamine.<sup>77</sup>

The flavin coenzyme in flavodoxin can be poised in one of three oxidation states: fully oxidized, semiquinone, or fully reduced. The unpaired electron in the semiquinone state is capable of severely broadening the resonance of any nucleus within 10 Å of the flavin ring. This was illustrated by the FMN phosphorus resonance being broadened beyond detection for the semiquinone form of flavodoxin, whereas the other two resonances were broadened negligibly. It could consequently be concluded that the two phosphoryl residues were remote from the FMN on the protein.<sup>77</sup>

The paramagnetic broadening effects were also employed in experiments with Mn(II) addition.<sup>77</sup> It was observed that the FMN peak is not broadened, but the phosphodiester peak was strongly broadened by Mn(II) in solution. Thus, it was concluded that the phosphodiester is near the protein surface and the FMN phosphate is buried.

## 2. Glucose Oxidase

Glucose oxidase from *Aspergillus niger* is a dimeric enzyme which contains 16% car-



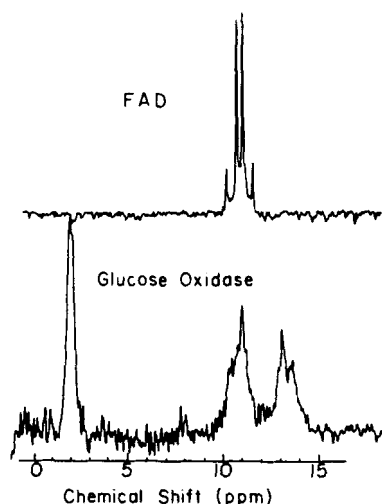


FIGURE 9.  $^{31}\text{P}$  NMR spectra (40.5 MHz) of (top) 10 mM FAD and (bottom) 1.7 mM glucose oxidase (oxidized form). The buffer was 100 mM Tris-acetate, pH 8.0, in both samples. Broadband proton decoupling was employed. From James, T. L., Edmondson, D. E., and Husain, M., *Biochemistry*, 20, 617, 1981. With permission.)

bohydrate, 1 mol of tightly bound flavin adenine dinucleotide (FAD), and 1 mol of a covalently bound phosphate residue per subunit. James et al.<sup>19</sup> have investigated  $^{31}\text{P}$  NMR spectra of glucose oxidase. The spectrum in Figure 9 shows the two FAD phosphorus resonances, coupled to one another, at about  $-11$  and  $-13$  ppm as well as the covalently bound phosphorus resonance. Reduction of the pH to 1.5, followed by Sephadex chromatography removed FAD. The spectrum of the resulting apoprotein at pH 8.5 in 3 M guanidinium chloride yielded a single resonance at  $-2.3$  ppm which is little different from that of the holoenzyme ( $-2.0$  ppm). In fact, the same shift was obtained for the phosphopeptide isolated on a Sephadex G-25<sup>®</sup> column following Pronase digestion.

The chemical shifts for both the holoenzyme and the phosphopeptide were invariant as the pH was lowered to pH 4.7.<sup>19</sup> As in the case of *Azotobacter* flavodoxin, this behavior implies that the phosphoryl group is disubstituted. The phospho bridge in glucose oxidase is illustrated in Figure 8. The identity of the participating amino acid residues is presently unknown, although we note that the chemical shift of  $-2.0$  ppm is not consistent with a phosphodiester bridge such as that in flavodoxin.

The disubstituted phospho group is protein bound rather than on the carbohydrate moiety judged by the following two observations: (1) periodate treatment removes the carbohydrate but not the phosphorus; and (2) Sephadex G-25<sup>®</sup> chromatography of the Pronase-digested glucose oxidase yields carbohydrate in the void volume and none in the phosphopeptide fraction.<sup>19</sup>

The flavin in native glucose oxidase was poised in the semiquinone and fully reduced states as well as the oxidized state. The unpaired electron in the FAD semiquinone form had little effect on the covalently bound phosphoenzyme signal implying that they were remote from one another.<sup>19</sup>

Addition of paramagnetic Mn(II) to the enzyme solution resulted in extensive broadening of the phosphoenzyme signal, but little broadening of the FAD resonances. This behavior suggests that, while the FAD is buried in the protein, the disubstituted phosphorus residue is near the surface.<sup>19</sup>

## REFERENCES

1. Cohn, M. and Nageswara Rao, B. D.,  $^{31}\text{P}$  NMR studies of enzymatic reactions, *Bull. Magn. Reson.*, 1, 38, 1979.
2. Vogel, H. J., Phosphorus-31 NMR studies of phosphoproteins, in  $^{31}\text{P}$  NMR: Principles and Applications, Gorenstein, D. G., Ed., Academic Press, New York, 1984, 105.
3. James, T. L., *Nuclear Magnetic Resonance in Biochemistry: Principles and Applications*, Academic Press, New York, 1975, 15.
4. Gorenstein, D. G., A generalized gauche NMR effect in  $^{13}\text{C}$ ,  $^{19}\text{F}$ , and  $^{31}\text{P}$  chemical shifts and directly bonded coupling constants. Torsional angle and bond angle effects, *J. Am. Chem. Soc.*, 99, 2254, 1977.
5. Lerner, D. B. and Kearns, D. R., Observation of large solvent effects on the  $^{31}\text{P}$  NMR chemical shifts of nucleotides, *J. Am. Chem. Soc.*, 102, 7611, 1980.
6. Vogel, H. J. and Bridger, W. A., Phosphorus-31 nuclear magnetic resonance pH titration studies of the phosphoproteins tropomyosin and glycogen phosphorylase *a*, *Can. J. Biochem.*, 61, 363, 1983.
7. Edmondson, D. E. and James, T. L., Covalently bound non-coenzyme phosphorus residues in flavoproteins:  $^{31}\text{P}$  nuclear magnetic resonance studies of *Azotobacter* flavodoxin, *Proc. Natl. Acad. Sci. U.S.A.*, 76, 3786, 1979.
8. Gassner, M., Stehlik, D., Schrecker, O., Hengstenberg, W., Maurer, W., and Rüterjans, H., The phosphoenolpyruvate-dependent phosphotransferase system of *Staphylococcus aureus* 2.  $^1\text{H}$  and  $^{31}\text{P}$  nuclear magnetic resonance studies on the phosphocarrier protein HPr, phosphohistidines and phosphorylated HPr, *Eur. J. Biochem.*, 75, 287, 1977.
9. Porubcan, M. A., Westler, W. M., Ibañez, I. B. and Markley, J. L., Diisopropylphosphorylserine proteinases. Proton and phosphorus-31 nuclear magnetic resonance-pH titration studies, *Biochemistry*, 18, 4108, 1979.
10. Blackburn, B. J., Lapper, R. D., and Smith, I. C. P., A proton magnetic resonance study of the conformations of 3',5'-cyclic nucleotides, *J. Am. Chem. Soc.*, 95, 2873, 1973.
11. Bolton, P. H., Investigation of phosphoserine and cytidine 5'-phosphate by heteronuclear two-dimensional spectroscopy: samples with strong proton coupling, *J. Magn. Reson.*, 45, 239, 1981.
12. Abragam, A., *Principles of Nuclear Magnetism*, Clarendon Press, Oxford, England, 1961, 295.
13. Kohler, S. J. and Klein, M. P.,  $^{31}\text{P}$  nuclear magnetic resonance chemical shielding tensors of phosphorylethanolamine, lecithin, and related compounds: applications to head-group motion in model membranes, *Biochemistry*, 15, 967, 1976.
14. Vogel, H. J., Bridger, W. A., and Sykes, B. D., Frequency-dependent phosphorus-31 nuclear magnetic resonance studies of the phosphohistidine residue of succinyl-CoA synthetase and the phosphoserine residue of glycogen phosphorylase *a*, *Biochemistry*, 21, 1126, 1982.
15. Terao, T., Matsui, S., and Akasaka, K.,  $^{31}\text{P}$  chemical shift anisotropy in solid nucleic acids, *J. Am. Chem. Soc.*, 99, 6136, 1977.
16. Nall, B. T., Rothwell, W. P., Waugh, J. S., and Rupprecht, A., Structural studies of A-form sodium deoxyribonucleic acid: phosphorus-31 nuclear magnetic resonance of oriented fibers, *Biochemistry*, 20, 1881, 1981.
17. Herzfeld, J., Griffin, R. G., and Haberkorn, R. A., Phosphorus-31 chemical-shift tensors in barium diethyl phosphate and urea-phosphoric acid: model compounds for phospholipid head-group studies, *Biochemistry*, 17, 2711, 1978.
18. Bendel, P. and James, T. L., Transverse relaxation of  $^{31}\text{P}$  in 5'-AMP, *J. Magn. Reson.*, 48, 76, 1982.
19. James, T. L., Edmondson, D. E., and Husain, M., Glucose oxidase contains a disubstituted phosphorus residue. Phosphorus-31 nuclear magnetic resonance studies of the flavin and nonflavin phosphate residues, *Biochemistry*, 20, 617, 1981.
20. Fung, B. M. and McGaughy, T. W., Cross relaxation in hydrated collagen, *J. Magn. Reson.*, 39, 413, 1980.
21. James, T. L., Relaxation behavior of nucleic acids. Dynamics and structure, in  $^{31}\text{P}$  NMR: Principles and Applications, Gorenstein, D. G., Ed., Academic Press, New York, 1984, 349.
22. Cohn, M.,  $^{18}\text{O}$  and  $^{17}\text{O}$  effects on  $^{31}\text{P}$  NMR as probes of enzymatic reactions of phosphate compounds, *Annu. Rev. Biophys. Bioeng.*, 11, 23, 1982.
23. Markley, J. L., Rhyu, G. I., and Ray, W. J., Jr., O-17 labeling of enzyme and substrate phosphates used to assign P-31 peaks and to probe mobilities of phosphate groups with phosphoglucomutase and its complexes, *Fed. Proc. Fed. Am. Soc. Exp. Biol.*, 41, 5069, 1982.
24. Bax, A., *Two-Dimensional Nuclear Magnetic Resonance in Liquids*, Delft University Press, Dordrecht, Holland, 1982.
25. Macura, S. and Ernst, R. R., Elucidation of cross relaxation in liquids by two-dimensional NMR spectroscopy, *Mol. Phys.*, 41, 95, 1980.
26. Bodenhausen, G. and Bolton, P. H., Elimination of flip angle effects in two-dimensional NMR spectroscopy. Application to cyclic nucleotides, *J. Magn. Reson.*, 39, 399, 1980.

27. Noggle, J. H. and Schirmer, R. G., *The Nuclear Overhauser Effect*, Academic Press, New York, 1971.
28. Kalk, A. and Berendsen, H. J. C., Proton magnetic relaxation and spin diffusion in proteins, *J. Magn. Reson.*, 24, 343, 1976.
29. Bothner-By, A. A. and Noggle, J. H., Time development of nuclear Overhauser effects in multispin systems, *J. Am. Chem. Soc.*, 101, 5152, 1979.
30. Olejniczak, E. T., Poulsen, F. M., and Dobson, C. M., Proton nuclear Overhauser effects and protein dynamics, *J. Am. Chem. Soc.*, 103, 6574, 1981.
31. Nicollai, N. and Tiezzi, E., Internal motions of aromatic amino acid side chains. Selective excitation nuclear relaxation and scalar coupling constant analysis on a model system, *J. Phys. Chem.*, 83, 3249, 1979.
32. Kuntz, I. D., Crippen, G. M., and Kollman, P. A., Application of distance geometry to protein tertiary structure, *Biopolymers*, 18, 939, 1979.
33. Wagner, G., Kumar, A., and Wüthrich, K., Systematic application of two-dimensional  $^1\text{H}$  nuclear-magnetic-resonance techniques for studies of proteins, *Eur. J. Biochem.*, 114, 375, 1981.
34. Kumar, A., Wagner, G., Ernst, R. R., and Wüthrich, K., Buildup rates of the nuclear Overhauser effect measured by two-dimensional proton magnetic resonance spectroscopy: implications for studies of protein conformation, *J. Am. Chem. Soc.*, 103, 3654, 1981.
35. Banaszak, L. J. and Seelig, J., Lipid domains in the crystalline lipovitellin/phosvitin complex: a phosphorus-31 and deuterium nuclear magnetic resonance study, *Biochemistry*, 21, 2436, 1982.
36. Schaefer, J. and Stejskal, E. D., High-resolution  $^{13}\text{C}$  NMR of solid polymers, in *Topics in Carbon-13 NMR Spectroscopy*, Vol. 3, Levy, G. C., Ed., Wiley-Interscience, New York, 1979, 284.
37. Griffin, R. G., Powers, L., and Pershan, P. S., Head-group conformation in phospholipids: a phosphorus-31 nuclear magnetic resonance study of oriented monodomain dipalmitoylphosphatidylcholine bilayers, *Biochemistry*, 17, 2718, 1978.
38. Pines, A., Gibby, M. G., and Waugh, J. S., Proton-enhanced NMR of dilute spins in solids, *J. Chem. Phys.*, 59, 569, 1973.
39. Barany, M. and Glonek, T., Phosphorus-31 nuclear magnetic resonance of contractile systems, *Methods Enzymol.*, 85, 624, 1982.
40. Bock, J. L. and Sheard, B.,  $^{31}\text{P}$  NMR of alkaline phosphatase, *Biochem. Biophys. Res. Commun.*, 66, 24, 1975.
41. Edmondson, D. E., personal communication.
42. Vogel, H. J. and Bridger, W. A., A phosphorus-31 nuclear magnetic resonance study of the intermediates of the *Escherichia coli* succinyl coenzyme A synthetase reaction, *J. Biol. Chem.*, 257, 4834, 1982.
43. Fossel, E., Post, R. L., O'Hara, D. S., and Smith, T. W., Phosphorus-31 nuclear magnetic resonance of phosphoenzymes of sodium- and potassium-activated and of calcium-activated adenosinetriphosphatase, *Biochemistry*, 20, 7215, 1981.
44. Gorenstein, D. G., Dependence of  $^{31}\text{P}$  chemical shifts on oxygen-phosphorus-oxygen bond angles in phosphate esters, *J. Am. Chem. Soc.*, 97, 898, 1975.
45. Goux, W. J., Perry, C., and James, T. L., An NMR study of  $^{13}\text{C}$ -enriched galactose attached to the single carbohydrate chain of hen ovalbumin, *J. Biol. Chem.*, 257, 1829, 1982.
46. Ho, C., Magnuson, J. A., Wilson, J. B., Magnuson, N. S., and Kurland, R. J., Phosphorus nuclear magnetic resonance studies of phosphoproteins and phosphorylated molecules. II. Chemical nature of phosphorus atoms in  $\alpha$ -casein B and phosvitin, *Biochemistry*, 8, 2074, 1969.
47. Kalbitzer, H. R. and Rösch, P., The effect of phosphorylation of the histidyl residue in the tetrapeptide Gly-Gly-His-Ala. Changes of chemical shift and pK values in  $^1\text{H}$ - and  $^{31}\text{P}$ -NMR spectra, *Org. Magn. Reson.*, 17, 88, 1981.
48. Oppenheimer, N. J., Singh, M., Sweeley, C. C., Sung, S.-J., and Srere, P. A., The configuration and location of the ribosidic linkage in the prosthetic group of citrate lyase (*Klebsiella aerogenes*), *J. Biol. Chem.*, 254, 1000, 1979.
49. Sleight, R. W., MacKinlay, A. G., and Pope, J. M., NMR studies of the phosphoserine regions of bovine  $\alpha_1$ - and  $\beta$ -casein. Assignment of  $^{31}\text{P}$  resonances to specific phosphoserines and cation binding studied by measurement of enhancement of  $^1\text{H}$  relaxation rate, *Biochim. Biophys. Acta*, 742, 175, 1983.
50. Humphrey, R. S. and Jolley, K. W.,  $^{31}\text{P}$ -NMR studies of bovine  $\beta$ -casein, *Biochim. Biophys. Acta*, 708, 294, 1982.
51. Vogel, H. J., Structure of hen phosvitin: a  $^{31}\text{P}$  NMR,  $^1\text{H}$  NMR, and laser photochemically induced dynamic nuclear polarization  $^1\text{H}$  NMR study, *Biochemistry*, 22, 668, 1983.
52. Linde, A., Bhowm, M., and Butler, W. T., Noncollagenous proteins of dentin, *J. Biol. Chem.*, 255, 5931, 1980.
53. Cookson, D. J., Levine, B. A., Williams, R. J. P., Jontell, M., Linde, A., and de Bernard, B., Cation binding by the rat-incisor-dentine phosphoprotein, *Eur. J. Biochem.*, 110, 273, 1980.
54. Bennick, A., McLaughlin, A. C., Grey, A. A., and Madapallimattam, G., The location and nature of calcium-binding sites in salivary acidic proline-rich phosphoproteins, *J. Biol. Chem.*, 256, 4741, 1981.

55. Chlebowski, J. F., Armitage, I. M., Tusa, P. P., and Coleman, J. E.,  $^{31}\text{P}$  NMR of phosphate and phosphonate complexes of metalloalkaline phosphatases, *J. Biol. Chem.*, 1207, 1976.
56. Hull, W. E., Halford, S. E., Gutfreund, H., and Sykes, B. D.,  $^{31}\text{P}$  nuclear magnetic resonance study of alkaline phosphatase: the role of inorganic phosphate in limiting the enzyme turnover rate at alkaline pH, *Biochemistry*, 15, 1547, 1976.
57. Chlebowski, J. F., Armitage, I. M., and Coleman, J. E., Allosteric interactions between metal ion and phosphate at the active sites of alkaline phosphatase as determined by  $^{31}\text{P}$  NMR and  $^{113}\text{Cd}$  NMR, *J. Biol. Chem.*, 252, 7053, 1977.
58. Bock, J. L. and Kowalski, A., Zinc stoichiometry in *Escherichia coli* alkaline phosphatase. Studies by  $^{31}\text{P}$  NMR and ion-exchange chromatography, *Biochim. Biophys. Acta*, 526, 135, 1978.
59. Otvos, J. D., Alger, J. R., Coleman, J. E., and Armitage, I. M.,  $^{31}\text{P}$  NMR of alkaline phosphatase. Saturation transfer and metal-phosphorus coupling, *J. Biol. Chem.*, 254, 1778, 1979.
60. Otvos, J. D., Armitage, I. M., Chlebowski, J. F., and Coleman, J. E.,  $^{31}\text{P}$  NMR of alkaline phosphatase. Dependence of phosphate binding stoichiometry on metal ion content, *J. Biol. Chem.*, 254, 4707, 1979.
61. Weiner, R. E., Chlebowski, J. F., Haffner, P. H., and Coleman, J. E., Mn(II) alkaline phosphatase. Electron spin resonance and  $^{31}\text{P}$  nuclear magnetic resonance, *J. Biol. Chem.*, 254, 9739, 1979.
62. Gettins, P. and Coleman, J. E.,  $^{31}\text{P}$  nuclear magnetic resonance of phosphoenzyme intermediates of alkaline phosphatase, *J. Biol. Chem.*, 258, 408, 1983.
63. Ray, W. J., Jr., Mildvan, A. S., and Grutzner, J. B., Phosphorus nuclear magnetic resonance studies of phosphoglucomutase and its metal ion complexes, *Arch. Biochem. Biophys.*, 184, 453, 1977.
64. Fletterick, R. J. and Madsen, N. B., The structures and related functions of phosphorylase *a*, *Annu. Rev. Biochem.*, 49, 31, 1980.
65. Withers, S. G., Madsen, N. B., and Sykes, B. D., Active form of pyridoxal phosphate in glycogen phosphorylase. Phosphorus-31 nuclear magnetic resonance investigation, *Biochemistry*, 20, 1748, 1981.
66. Hoerl, M., Feldman, K., Schnackerz, K. D., and Helmreich, E. J., Ionization of pyridoxal 5'-phosphate and the interactions of AMP-S and thiophosphoseryl residues in native and succinylated rabbit muscle glycogen phosphorylase b and a as inferred from  $^{31}\text{P}$  NMR spectra, *Biochemistry*, 18, 2457, 1979.
67. Sperling, J. E., Feldman, K., Meyer, H., Jahnke, U., and Hellmeyer, L. M. G., Isolation, characterization, and phosphorylation pattern of the troponin complexes  $\text{Ti}_2\text{C}$  and  $\text{I}_2\text{C}$ , *Eur. J. Biochem.*, 101, 581, 1979.
68. Koppitz, B., Feldmann, B., and Hellmeyer, L. M. G., The P-light chain of rabbit skeletal muscle myosin: a  $^{31}\text{P}$  NMR study, *FEBS Lett.*, 117, 199, 1980.
69. Vogel, H. J. and Bridger, W. A., Phosphorus-31 nuclear magnetic resonance studies of the two phosphoserine residues of hen egg white ovalbumin, *Biochemistry*, 21, 5825, 1982.
70. Mueller, D. B., Kramer, K. J., and Bolden, T. D., Phosphorus-31 nuclear magnetic resonance of insect hemolymph sera, *Arch. Biochem. Biophys.*, 210, 64, 1981.
71. Buttlare, D. H., Cohn, M., and Bridger, W. A., Interactions of phospho- and dephosphosuccinyl coenzyme A synthetase with manganous ion and substrates, *J. Biol. Chem.*, 252, 1957, 1977.
72. Dooijewaard, G., Roossien, F. F., and Robillard, G. T., *Escherichia coli* phosphoenolpyruvate dependent phosphotransferase system. NMR studies of the conformation of HPr and P-HPr and the mechanism of energy coupling, *Biochemistry*, 18, 2996, 1979.
73. Kalbitzer, H. R., Deutscher, J., Hengtenberg, W., and Rösch, P., Phosphoenolpyruvate-dependent phosphotransferase system of *Staphylococcus aureus*:  $^1\text{H}$  nuclear magnetic resonance studies on phosphorylated and unphosphorylated factor III<sup>ac</sup> and its interaction with the phosphocarrier protein HPr, *Biochemistry*, 20, 6178, 1981.
74. Fujitaki, J. M., Fung, G., Oh, E. Y., and Smith, R. A., Characterization of chemical and enzymatic acid-labile phosphorylation of histone H4 using phosphorus-31 nuclear magnetic resonance, *Biochemistry*, 20, 3658, 1981.
75. Perlman, G. E., Enzymic dephosphorylation of pepsin and pepsinogen, *J. Gen. Physiol.*, 41, 441, 1958.
76. Clement, G. E., Rooney, J., Zakheim, D., and Eastman, J., The pH dependence of the dephosphorylated pepsin-catalyzed hydrolysis of *N*-acetyl-L-phenylalanyl-L-tyrosine methyl ester, *J. Am. Chem. Soc.*, 92, 186, 1970.
77. Edmondson, D. E. and James, T. L., Physical and chemical studies on the FMN and non-flavin phosphate residues in *Azotobacter flavodoxin*, in *Flavins and Flavoproteins*, Massey, V. and Williams, C. H., Eds., Elsevier/North-Holland, Amsterdam, 1982, 111.